REDUCING PM CONCENTRATIONS IN SIMULATED HIGH TEMPERATURE GAS STREAMS

A Thesis

by

DANIEL ROBERT LUEHRS

Submitted to the Office of Graduate and Professional Studies of
Texas A&M University
in partial fulfillment of the requirements for the degree of

MASTER OF SCIENCE

Chair of Committee,	Calvin B. Parnell, Jr.
Committee Members,	Sergio C. Capareda
	Jorge L. Alvarado
Head of Department,	Stephen W. Searcy

August 2014

Major Subject: Agricultural Systems Management

ABSTRACT

The goal of this research is to use the energy in cotton gin trash (CGT) to fuel an internal combustion engine (ICE) driving a generator to produce electricity for a cotton gin. CGT is a fuel that has char that melts at low temperatures. This characteristic is referred to as char having a low eutectic point. Biomasses with low eutectic points cannot be used in a combustion process because the char will result in slagging and fouling. We have used fluidized bed gasification (FBG) to control the reaction temperatures and capture the energy in the biomass. CGT has an approximant 16,300 kJ/kg (7,000 Btu/lb) of energy. The resulting synthetic gas (syngas) can have an energy content as high as 7,450 kJ/m^3 (200 Btu/dscf) and can be fed directly into an internal combustion engine (ICE) which can drive a generator to produce electricity. The syngas conveys the char from the bed to the gas cleanup system consisting of specially designed cyclones. The cyclones were used to reduce particulate matter (PM) concentrations in the syngas prior to delivery to the ICE. Cyclones are capable of reducing the concentrations of particulate matter from syngas streams. The temperatures of the syngas leaving the gasification bed ranges from 371 to 760 ºC (700 to 1400 ºF). These high temperatures impact the cyclone inlet velocities as a consequence of the reduced gas densities. Changes in gas densities will influence the cyclone design. It was hypothesized that changes in cyclone performances as a consequence lower gas densities could be approximated by increasing the cyclones inlet velocities of air at standard temperature and pressure (STP) to correspond to the anticipated cyclone's inlet velocities of syngas at the higher temperatures. Multiple tests of cyclone performances in simulated high

temperature gas streams were conducted using bio-char. Preliminary cyclone testing results indicate that the location of the vortex inverter in the cyclone relative to the natural length can significantly impact the cyclone performance and design. Tests were conducted at inlet velocities of 16.3, 30.5, and 45.7 m/s (3,000, 6,000 and 9,000 fpm). Increasing inlet velocities resulted in increasing the cyclone's natural length. This study was limited to testing cyclone performances at ambient temperatures and simulating high temperature airflow rates and velocities for safety purposes. Natural lengths were used to help determine the optimum location of the vortex inverter; resulting in a new design process for cyclones operating with high temperature gases.

DEDICATION

To God, Mom and Dad, Dr. Parnell, and Russell McGee.

ACKNOWLEDGEMENTS

I would like to acknowledge everyone who had a part in getting me to this point in my life. From my family and friends to co-workers and bosses for raising me to be the man I have become. To name them all would make a list longer than this thesis, but I want it to be known that I appreciate everyone who has been a part of my upbringing.

As a kid, I was taught values and morals from my parents and grandparents, which in time shaped my work ethic. For that, I would like to thank my parents, Robert and Joy Luehrs, and my grandparents, Lester and Marguerite Luehrs and Fed and Jean McAnear.

At Texas A & M University I have had the chance to learn and grow thanks to the support from professors like Dr. Calvin Parnell, Col. Russell McGee, Dr. Brock Faulkner, and Lt. Col. Chris Emmerson. The men I have listed have given me the opportunity, support, and knowledge to make it to this point in my academic career. I am especially thankful for the Cotton Chair, Dr. Parnell, for the opportunity to study at Texas A & M.

My work in graduate school could not have been completed without the help from my co-workers in the CAAQES lab: Shane Saucier, Balaji Ganesan, Jordan Grier, Zach Skrabanek, David Arthur, Kyle Birkenfeld, Walter Oosthuizen, and Demi Dean.

Most importantly I am thankful for a loving God who has made all of the above possible and the love and support from my brother and sister.

NOMENCLATURE

AED	Aerodynamic Equivalent Diameter
BAEN	Biological and Agricultural Engineering
CCD	Classical Cyclone Design
CGT	Cotton Gin Trash
^oC	Degrees Celsius
D	Cyclone Diameter
D_o	Diameter Of Cyclone Outlet
D_s	Diameter Of Outer Vortex Strand
d_{50}	Particle Size At 50% Greater/Less
d_{pc}	Cutpoint
ΔP	Pressure Drop
ΔP_e	Pressure Drop Due To Entrance
ΔP_f	Pressure Drop Due To Friction
ΔP_{fi}	Pressure Drop Due To Friction In One Turn
ΔP_k	Pressure Drop Due To Kentic Energy
ΔP_o	Pressure Drop Due To Outlet
ΔP_Q	Orifice Meter Pressure Drop
dscm	Dry Standard Cubic Meter
η	Collection efficiency
f	Friction Factor
FBG	Fluidized Bed Gasification

FEC	Fractional Efficiency Curve
GSD	Geometric Standard Deviation
H_c	Height of Cyclone Inlet
ICE	Internal Combustion Engine
K	Constant for Cyclone Pressure Drop Calculations
kPa	Kilopascals
K_Q	Constant for Orifice Meter
L	Outer Vortex Travel Distance
L_b	Length of Cyclone Barrel
L_c	Length of Cyclone Cone
L_N	Natural Length
LCV	Low Calorific Value
LFE	Laminar Flow Element
M_c	Mass Captured by the Cyclone
M_f	Mass Captured by the Filter
μ	Viscosity
μm	Micrometers
MJ	Mega Joule
MMD	Mass Median Diameter
MW	Megawatt
N_e	Number of Turns
PM	Particulate Matter

PSD	Particle Size Distribution
ρ_a	Density of Air
ρ_g	Density of Gas
ρ_p	Density of Particles
Q	Airflow Rate
Re	Reynolds Number
RPM	Revolutions per Minute
STP	Standard Temperature and Pressure
syngas	Synthesis Gas
TAMU	Texas A&M University
TCD	Texas A&M University Cyclone Design
TCGA	Texas Cotton Ginners Association
V_i	Inlet Velocity
V_o	Outlet Velocity
V_s	Strand Velocity
VP_i	Inlet Velocity Pressure
VP_o	Outlet Velocity Pressure
VP_s	Strand Velocity Pressure
W	Width of the Cyclone Inlet

TABLE OF CONTENTS

Page

Page

LIST OF FIGURES

Page

Page

LIST OF TABLES

Page

Page

CHAPTER I

INTRODUCTION AND LITERATURE REVIEW

Fluidized-Bed Gasification (FBG) is a proposed renewable energy solution for cotton gins as the demand for electricity from the grid increases. Currently, cotton gins require 108 to 180 MJ (30 to 50 kW-h) to produce a bale of cotton (Texas Cotton Ginners Association, 2006). The faculty members in the department of Biological and Agricultural Engineering (BAEN) at Texas A&M University (TAMU) have been conducting research on FBG of biomasses, including cotton gin trash (CGT) for a number of years. The goals of FBG research were to produce a synthetic gas (syngas) that could be used to produce electricity (Capareda and Parnell, 2007; Parnell, 1985).

The first patent on the TAMU gasifier was in 1989 (US Patent No. 4848249) and the second was a 2010 provisional patent (Serial No. 61/302,001) that incorporated cyclones in series for biochar removal. The design concept was to have the first cyclone remove the large particles and the second cyclone to remove the smaller particles.

FBG is a thermo-chemical reaction converting a biomass into two products in the exiting gas stream: syngas and bio-char. Syngas comprises 80% of the mass in the gas stream and bio-char comprises the remaining 20%. The FBG system is void of oxygen, with regulated energy loading rates and fuel-to-air ratios.

CGT is a low eutectic biomass, meaning that the ash/char produced has a low melting point. Melting ash/char will result in slagging and fouling. FBG allows for

controlling the temperature to levels below those resulting in problems (LePori, et al., 1985).

CGT has an energy content of approximately 16.3 MJ/kg (7,000 Btu/lb.). The syngas produced can have an energy content of 7,450 kJ/dry standard cubic meter (dscm) (200 Btu/dscf). A syngas fueled internal combustion engine (ICE) has an estimated capital cost of $1 million per MW as opposed to $2 million per MW for the boiler/steam turbine concept (Capareda et al. 2010).

Maglinao (2013) reported on the utilization of syngas to operate a spark ignition engine generator. It was observed that the fuel line ductwork and spark plugs were being clogged with char after two-hour tests. He suggested that clogging could be prevented by efficiently removing particles from the syngas. There are different design process that can be used to sizes cyclones.

Wang (2004) describes the Classical Cyclone Design (CCD) and the TAMU Cyclone Design (TCD) as two methods used to design cyclones. The CCD method is also described in Cooper and Alley (2011).

In the CCD process, an optimum dimension was used to size cyclones base on the body diameter (Cooper and Alley, 2011). The optimum dimensions of a cyclone were decided by choosing the diameter that yields the collection efficiency required. The CCD method for solving for the cyclone collection efficiency was determined by finding the cut point in equation 1 (Lapple, 1951):

$$d_{pc} = \sqrt{\frac{9\mu W}{2\pi N_e V_i (\rho_p + \rho_g)}} \quad (1)$$

where,

d_{pc} = cyclone cutpoint (μm),

μ = gas viscosity (kg/m-s),

W = width of cyclone inlet (m),

N_e = number of turns,

V_i = inlet velocity (m/sec),

ρ_p = particle density (kg/m^3), and

ρ_g = gas density (kg/m^3).

However, the CCD method uses a flawed efficiency equation. Results of recent studies have shown that the TCD process more accurately predicts cyclone efficiencies by moving the 2 in the denominator outside of the radical (Faulkner et al., 2008).

Both methods can be used to determine the predicted number of turns. The CCD method uses equation 2 to determine the number of turns in a cyclone (Lapple, 1951):

$$N_e = \frac{1}{H_c}\left[L_b + \frac{L_c}{2}\right] \quad (2)$$

where,

N_e = number of effective turns,

H_c = height of inlet duct (m),

L_b = length of barrel body (m), and

L_c = vertical length of cone body (m).

In the TCD process the cyclone is sized based upon a design inlet velocities. There are a predetermined number of turns depending on the cyclone design. The number of turns in a cyclone using this approach is listed in table 1 (Parnell, 1996).

Table 1: The design inlet velocity and number of turns for a cyclone in the TCD process.

Cyclone	Inlet Velocity (±2.03 m/s)	Number of turns
1D3D	16.3 m/s (3,200 fpm)	6
2D2D	15.2 m/s (3,000 fpm)	6
1D2D	12.2 m/s (2,400 fpm)	2.3

The pressure drop calculation for both methods requires the designer to utilize a constant, K. The K value is based upon the cyclone configuration and operating conditions. The TCD process for calculating pressure drop utilizes inlet and outlet velocity pressures.

LePori and Soltes (1985) reported cyclone efficiencies for the separation of bio-char from syngas from the initial gasification system. The separation of biochar from the syngas stream was accomplished with TCD 1D3D cyclone in series with a 1D5D cyclone. The reported efficiencies approached 97% for removing biochar concentrations from the syngas.

Simpson and Parnell (1996) reported efficiencies for the TCD 1D3D and 1D2D cyclones up to 99%. Particulate matter (PM) used was found in agricultural industries with typical concentrations of 6 grams per cubic meter (g/m^3). These concentrations were much lower than the encountered concentrations of 160 g/m^3 in the exiting gas stream of FBG (LePori and Soltes, 1985).

Saucier (2013) tested cyclone collection efficiency for FBG of CGT. He found that a 1D3D cyclone was capable of separating an average of 97% of the bio-char from air at STP. He tested cyclone performance at concentrations of bio-char ranging from 56

to 136 g/m^3. Additional findings showed that as the bio-char concentration in the gas increased the pressure drop decreased, following Shepherd and Lapple's (1939) assumption. Saucier reported that two cyclones were not needed and suggested that one cyclone could be used in FBG systems.

Wang et al. (2006) conducted a study comparing methods for calculating cyclone pressure drops. In the study, she conducted experiments to verify a theoretical approach for calculating pressure drop across cyclones. The other pressure drop equations compared in this study belonged to First (1950), Alexander (1949), Stairmand (1949), Barth (1956), and Shepherd and Lapple's (1939, 1940) empirical CCD approach. Among all the models, Wang's theoretical approach and the Alexander model had the best representation of the experimental pressure drop. Wang's approach determined the number of turns by using average velocity and travel distance.

Simpson (1996) found that as the inlet velocity of the cyclone increased the efficiency would decrease. A 1D2D cyclone was recorded to have an existing concentration go from 100 mg/m^3 at 14.2 m/s (2,800 fpm) to 343 mg/m^3 at 16.3 m/s (3,200 fpm). A range of 2.03 m/s was established above or below the optimal design velocity to achieve the highest cyclone efficiency.

All of the previous TCD cyclone work has been within a range that can be considered ambient conditions. However, the operating conditions of FBG are outside the range of ambient conditions.

FBG Project Description

Previous test results produced by Saucier (2013) were helpful in the planning of tests for this research. The following findings were used to construct the test apparatus and plan the tests.

- The temperatures of the syngas leaving the gasification bed ranged from 538 to 760ºC (1,000 to 1,400ºF).
- The syngas temperatures entering the cyclone were typically 371 to 538ºC (700 to 1,000ºF).
- The energy loading of the gasifier had an upper limit of 23,900 MJ/m^2-hr (2.1 MMBtu/ft^2-hr).
- The fuel- to- air ratio was controlled at one pound of fuel per pound of gases:
- The bed area was 0.0186 m^2 (0.2 ft^2).

The resulting temperatures in the gasifier resulted in reduced gas densities and thus increased the inlet velocities of the cyclones. It was hypothesized that the changes in cyclone performance could be measured by testing cyclones at STP with inlet velocities corresponding to those associated with syngas densities at high temperatures. The inlet velocity of the cyclone was calculated using the ideal gas law to solve for the gas density given the temperature. In this research, tests were conducted to evaluate cyclone emission concentrations and pressure drops with three inlet velocities to simulate the syngas density at high temperatures. The inlet velocities, shown in table 2, correspond to syngas temperatures at STP and the upper and lower range seen from FBG.

Table 2: Approximate inlet velocities of air at STP used to simulate inlet velocities of high temperature gases. As the temperature increases the density of the syngas decreases.

Related Temperature (°C)	Related Density (kg/m^3)	Inlet Velocity (m/s)
21	1.20	16.3
94	0.96	20.3
187	0.77	25.4
278	0.64	30.5
371	0.55	35.6
462	0.48	40.6
554	0.43	45.7

Increased inlet velocities affect the cyclone's natural length. The term natural length describes the vertical length the air stream travels down the body of the cyclone. This distance spans from the top of the inlet to the turning point where the outer vortex (outer air stream) changes direction moving upward into the inner vortex (inner air stream). Hoffmann (1995) observed a varying natural length at higher velocities. He recommended that the cyclone collection efficiency would be highest the closer the natural length was to the physical length.

Tullis (1997) tested barrel cyclone efficiencies with varying vortex inverters. The function of the vortex inverter is to turn the outer vortex inward to the inner vortex. The vortex inverter location defines the physical length of the cyclone. The physical length is the distance from the top of the cyclone's inlet to the top of the vortex inverter.

The PM to be used in this cyclone system is bio-char from the gasification of sweet sorghum. The bio-char's particle size distributions (PSDs) are best defined by lognormal distributions defined by mass median diameters (MMDs) and geometric

standard deviations (GSDs) (Cooper and Alley, 2011). The lognormal fit of the measured and theoretical PSDs, obtained using the Coulter Counter, are shown in figure 1. The biochar Saucier (2013) used had a MMD aerodynamic equivalent diameter (AED) of 34 µm, a geometric standard deviation (GSD) of 2.2 and a particle density of 2.1 g/cm^3.

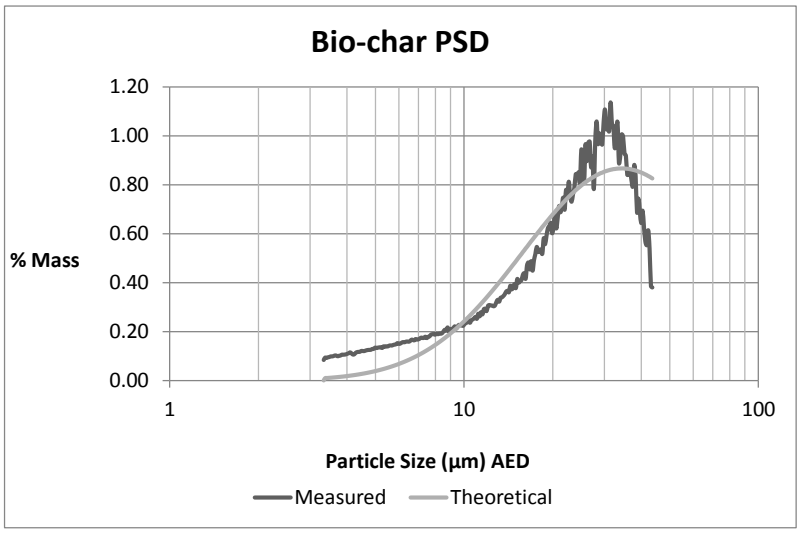

Figure 1: Particle size distributions of bio-char. The measured PSD was obtained using a Coulter Counter.

Research Goals

The goal of this work was to determine a cyclone that minimizes the bio-char

concentrations from high temperature gas streams. The goal was achieved by developing and completing the following objectives:

- Construct a testing system to simulate the anticipated volumetric flow rate and bio-char concentrations leaving a FBG reactor bed at high temperatures.
- Determine the optimal vortex inverter placement at a range of inlet velocities.
- Maximize bio-char removal from simulated FBG gas streams.

CHAPTER II

MATERIALS AND METHODS

Tests for the cyclones natural length and cyclone collection efficiency were run and recorded separately. The results from determining the cyclone's natural length were planned to be used in consideration in the design of the cyclone for collection efficiency testing. A testing system for each objective was constructed.

Cyclone Visualization Testing System

The testing system shown in figure 2 was designed and constructed to visualize the number of turns and natural length of a cyclone. Both Luehrs (2014) and Hoffmann (1995) recorded a liquid ring marking the turning point when solutions were injected into the cyclone. Identification of the turning point allowed for the measurement of the natural length.

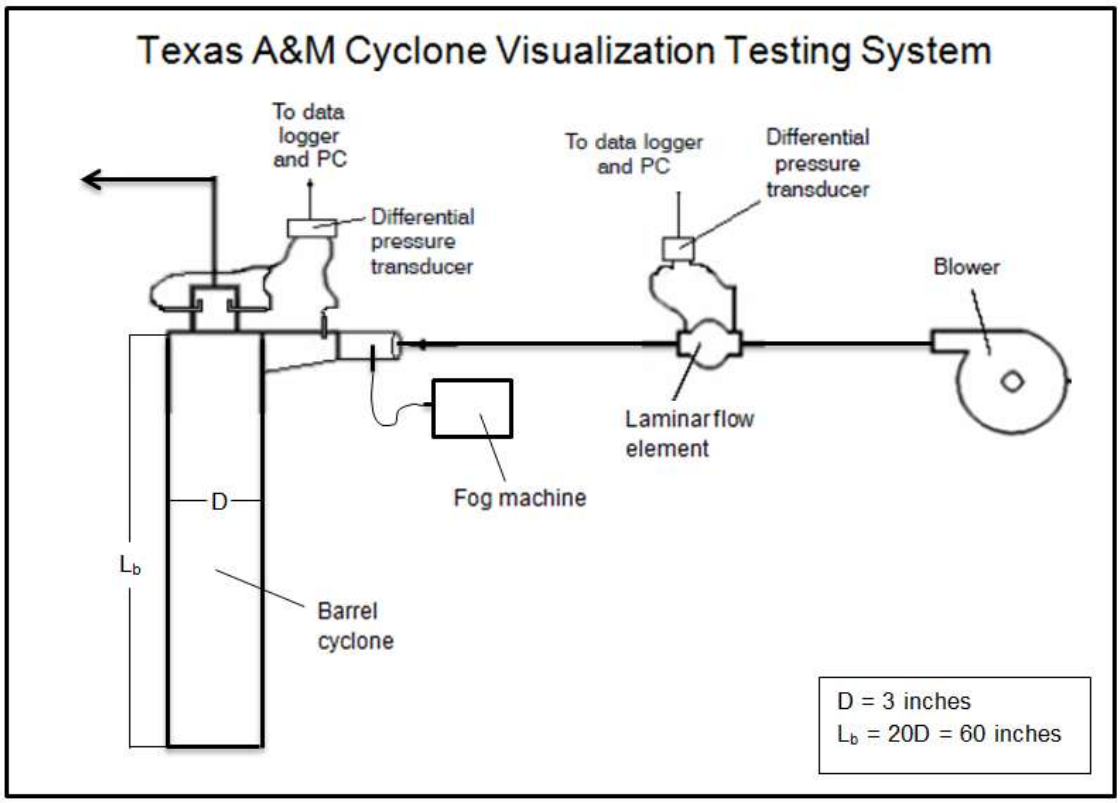

Figure 2: The Texas A&M cyclone visualization testing system.

Airflow to the cyclone was accomplished by using an automated vacuum pump (3 in. Legend Series Positive Displacement Vacuum Pump, Sutorbilt, Gardner Denver, IL). The desired flow was monitored with an orifice meter. This pump could operate at 3,600 rpm under 96.5 kPa of vacuum pressure.

An orifice meter was designed and built to operate on a scale of 0.249 to 2.49 kPa (1 to 10 in. w.g.) for airflow from 34 to 127 m^3/hr (20 to 75 cfm). A laminar flow element was used to calibrate the orifice meter. Pressure drops detected by the orifice meter were recorded utilizing a Dwyer Magnesense differential Pressure Transmitter. Data Points were collected every 10 seconds during testing.

Inlet velocities were calculated by measuring airflow through the orifice meter. The differential pressure, over the orifice meter, was recorded and used to monitor the system airflow rate by the following relationship in equation 3:

$$Q = 3.478\ K_Q\ D_o^2 \sqrt{\frac{\Delta P_Q}{\rho_a}} \quad (3)$$

where,

Q = airflow rate (m^3/s),

K_Q = flow coefficient (dimensionless) (0.539),

D_o = orifice diameter (3.29 cm),

ΔP_Q = pressure drop cross the orifice (mm H_2O), and

ρ_a = air density (1.2 kg/m^3).

Pressure drop across the cyclone was recorded utilizing a Dwyer Magnesense differential Pressure Transmitter. Static pressure was recorded at the inlet and the outlet of the cyclone. The pressure tap in the exit tube was centered in order to reduce the interference of velocity pressure. Data Points were collected every 10 seconds during testing.

Models

Wang published a model for a theoretical approach to calculate the pressure drop across a cyclone that incorporated inlet velocity and travel distance (Wang et al., 2002 and 2006). Her model utilized components of pressure drop. The equations used in the TCD process are the accumulation of the factors that comprise the pressure drop inside of the cyclone. However, the pressure drop component due to the radial forces, in the

cone section of the cyclone, was omitted from this model. The total pressure drop can be calculated using equation 4:

$$\Delta P = \Delta P_e + \Delta P_k + \Delta P_o + \Delta P_f \quad (4)$$

where,

ΔP = total cyclone pressure drop (kPa),

ΔP_e = cyclone entry loss, equal to C_e*VP_i ($C_e \approx 1$) (kPa),

ΔP_k = kinetic energy loss, VP_i - VP_o (kPa),

ΔP_o = outlet and inner vortex energy loss, equal to C_o*VP_o ($C_o \approx 1.8$) (kPa), and

ΔP_f = frictional energy loss, function of natural length (kPa).

The total pressure drop and three of the components (ΔP_e, ΔP_k, and ΔP_o) were calculated. The portion of pressure drop loss due to friction was treated as the unknown variable. Assuming a constant vertical trajectory of the outer vortex, the frictional force was used to estimate the number of turns and natural length.

Cyclone Efficiency Testing System

The test system shown in figure 3 was designed and constructed to test cyclone efficiencies. Bio-char was fed into the airstream prior to reaching the cyclone. Char entering the cyclone was either captured by the cyclone and fell into the char hopper or remained in the exiting airstream was it was captured in the filter assembly. A positive displacement pump provided the airflow in the system. The airflow was monitored by an orifice meter. Differential pressure gauges measured the pressure drop across the cyclone and orifice meter.

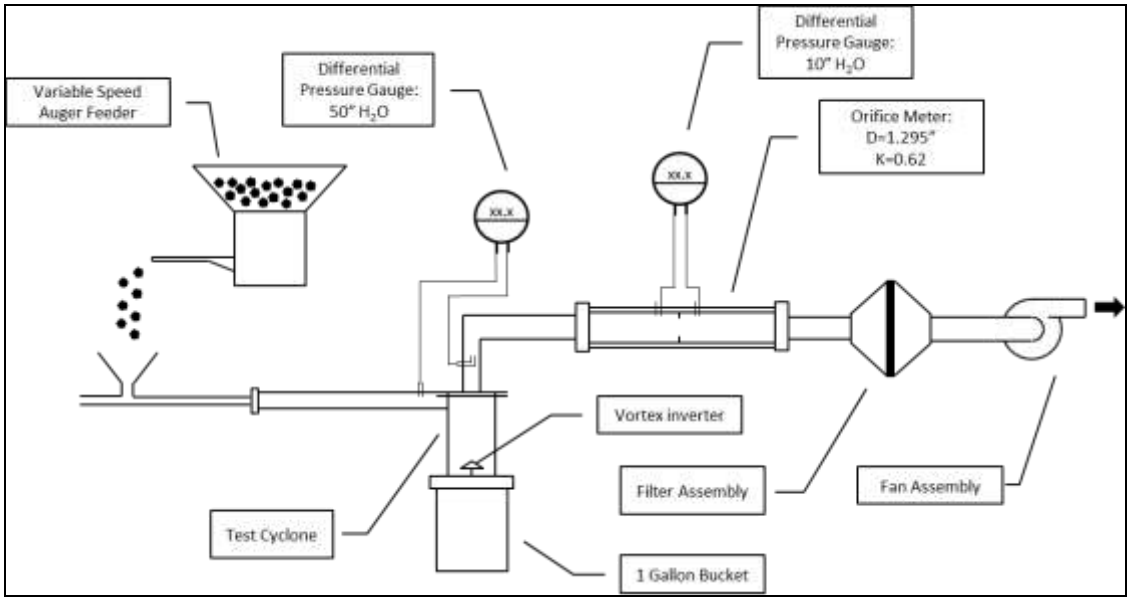

Figure 3: Cyclone collection efficiency testing system.

Bio-char was fed in to the system with a 0.635 cm variable speed auger. The feeder has agitators inside of the hopper above the auger to prevent the bio-char from bridging. Achievable feed rates range from 5 to 120 g/min. The bio-char was sieved to below 100 μm prior to testing.

The vortex inverter had a diameter of 0.9D and a height of 0.45D (Tullis, et al., 1997). The vortex inverter was adjustable, allowing the ability to vary the physical length of the cyclone for higher inlet velocities.

Glass–fiber filters (G810, Graseby GMW, Smyrna, Ga.) were used for collection of bio-char exiting the cyclone. Glass fiber filters are relatively inert and non-hygroscopic. The filters were weighed before and after sampling with a high–precision analytical balance (AG245, Mettler Toledo, Greifensee, Switzerland).

Texas A&M Cyclone Design Process

The TCD process states the performance of a cyclone is defined by its fractional efficiency curve (FEC), which indicates the efficiency with which a cyclone collects particles of a given size (Faulkner et al., 2008). An ideal FEC is characterized a lognormal distribution defined by the cutpoint and slope. The TCD process determines the cyclone cut point by equation 5:

$$d_{pc} = \frac{1}{2}\sqrt{\frac{9\mu W}{\pi N_e V_i(\rho_p+\rho_g)}} \quad (5)$$

where,

d_{pc} = cyclone cutpoint (μm),

μ = gas viscosity (kg/m-s),

W = width of inlet (m),

N_e = number of turns,

V_i = inlet velocity (m/sec),

ρ_p = particle density (kg/m^3), and

ρ_g = gas density (kg/m^3).

The slope in the FEC is equal to sharpness of collection efficiency from d_{50} to $d_{15.9}$ and $d_{84.1}$. An example FEC is shown in figure 4 (Faulkner et al., 2008).

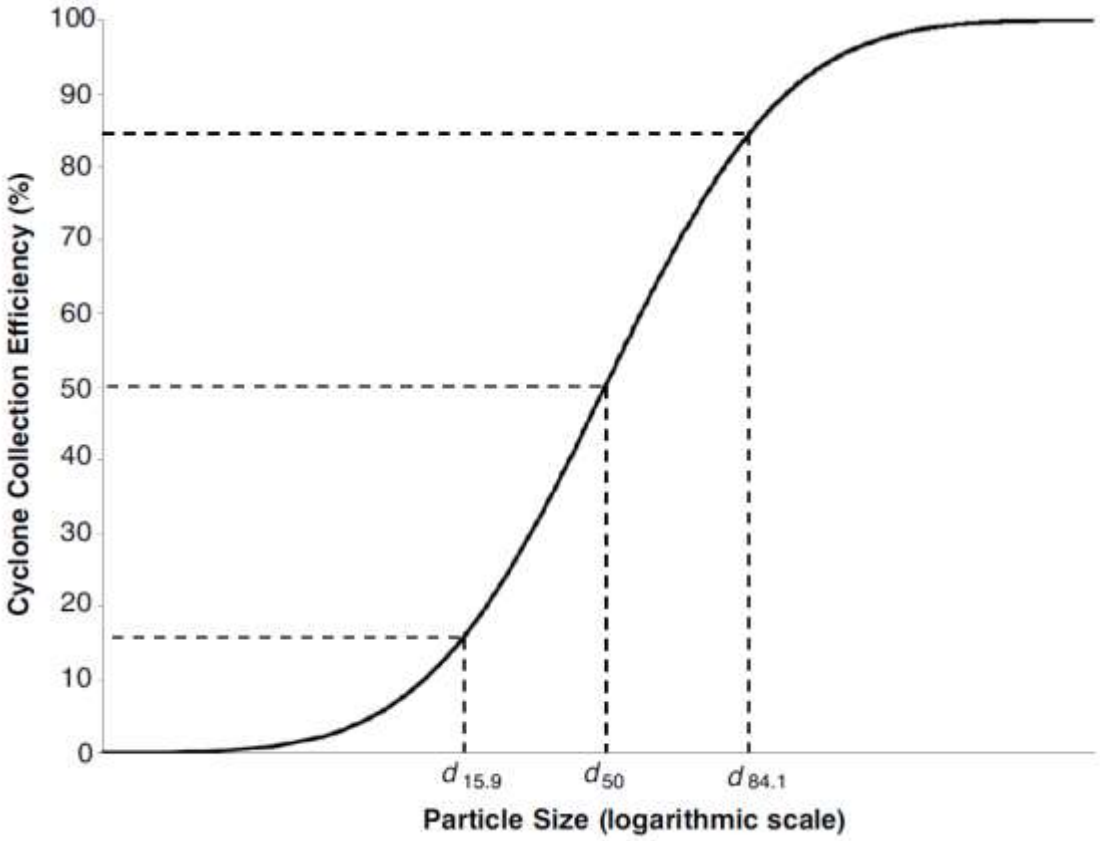

Figure 4: Fractional efficiency curve.

Due to the design and application of this cyclone, there is not currently a defined slope. Previous cyclone work was able to define a cutpoint and slope for each of the TCD cyclones. Cyclones tested with fly ash were recorded as the most conservative results and can be seen in table 3 (Wang, 2004).

Table 3: TCD cyclone cutpoint and slope to be used in FEC's.

Cyclone	Cutpoint (μm)	Slope
1D3D	4.25	1.2
2D2D	4.40	1.2
1D2D	4.50	1.3
Barrel	4.60	1.3

Pressure drop was estimated by following equation 6 in the TCD process:

$$\Delta P = K(VP_i + VP_o) \quad (6)$$

where,

ΔP = total cyclone pressure drop (kPa),

K = cyclone pressure drop factor,

VP_i = velocity pressure of the inlet (kPa), and

VP_o = velocity pressure of the outlet (kPa).

Velocity pressure of the inlet was determined with equation 7:

$$VP_i = \frac{1}{2} V_i^{\,2} \rho_a \quad (7)$$

where,

VP_i = inlet velocity pressure (kPa),

V_i = inlet velocity (m/s), and

ρ_a = density of gases (kg/m^3).

Velocity pressure of the inlet was determined with equation 8:

$$VP_o = \frac{1}{2} V_o^{\,2} \rho_a \quad (8)$$

where

VP_o = outlet velocity pressure (kPa),

V_o = outlet velocity ($2V_i/\pi$) (m/s), and

ρ_a = density of gases (kg/m^3).

Cyclone Efficiency Testing Procedure

The PM captured by the cyclone, removed from the airstream, was referred to as M_c, mass captured by the cyclone. PM not captured by the cyclone, or remaining in the airstream, had to be measured to determine efficiency. Common practice in cyclone testing is to capture all PM in the exiting airstream with a filter assembly. The PM captured by the filter assembly exiting the cyclone was referred to as M_f, mass captured by the filter. The cyclone collection efficiency was calculated by equation 9:

$$\eta = \frac{M_c}{M_c + M_f} \times 100\% \quad (9)$$

where,

η = collection efficiency of the cyclone (%),

M_c = mass captured by the cyclone (g), and

M_f = mass captured by the filter (g).

The filters are capable of capturing 0.167 g/m^2 (one gram per filter). It was recorded that the airflow through the system would start to decrease due to the rapid increase in system static pressure as the filter became loaded and the duration of the test for the cyclone would be limited to only a few minutes (Faulkner et al., 2008). Luehrs (2014) reported similar filter concentration levels would result in system pressure drop. The criterion given to determine when the filter has reached capacity, and the test should end, was when the inlet velocity of the cyclone dropped 2.03 m/s (400 fpm). This level is the low end of the TCD recommended inlet velocity range (Wang et al., 2002). A 2.03

m/s decrease in the inlet velocity of the cyclone equates to a 149.4 Pa (0.6 in. w.g) pressure drop over the orifice meter.

The known capabilities of the filters are used to determine the filter configuration. Load rates were chosen based on their feasibility and relationship to FBG. The design used filters to capture the exiting bio-char concentration from the cyclone. The exiting concentration was determined by the mass collected on the filter over a period of time given the airflow rate.

Tests were conducted in a randomized complete block design with four replicates. Averages and standard deviations were taken for all data recorded. Data outside of three standard deviations from the average is considered an outlier and was removed. Seven inlet velocities were used to measure the natural length. Following procedures from Luehrs (2014), three inlet velocities were used to determine the cyclone collection efficiency. The bio-char concentrations at each inlet velocity can be seen in table 4.

Table 4: The table shows the expected inlet concentrations with a loading rate of 20 g/min at three inlet velocities for the cyclone.

Inlet Velocity (m/s)	Inlet Concentration (g/m^3)
16.3	28.2
30.5	15.1
45.7	10

Tests for the cyclones natural length and cyclone collection efficiency were run and recorded separately. This was done because the results from determining the cyclone's natural length were used in testing the cyclone's efficiency.

CHAPTER III

VISUALIZATION RESULTS AND DISCUSSION

The goal of this study is to remove PM in high temperature gases from FBG. Due to the feasibility of testing cyclones at temperatures above ambient conditions all test were conducted with an airflow rate at STP that can represent the high temperature gases.

The temperatures of the syngas leaving the gasification bed ranges from 538 to 760ºC (1,000 to 1,400ºF). The syngas temperature entering the cyclone was typically 371 to 538ºC (700 to 1,000ºF). The energy loading of the gasifier has an upper limit of 23,900 MJ/m^2-hr (2.1 MMBtu/ft^2-hr). The fuel- to- air ratio was 1:1. The bed area was 0.0186 m^2 (0.2 ft^2).

The testing system shown in figure 2 was designed and constructed to visualize the number of turns and natural length of a cyclone. A positive displacement pump provided the airflow in the system. The airflow was monitored by an orifice meter. Differential pressure gauges measured the pressure drop across the cyclone and orifice meter.

The reduced gas densities increased the inlet velocities of the cyclones. It was hypothesized that the changes in cyclone performance could be measured by testing cyclones at STP with inlet velocities corresponding to those associated with syngas densities at high temperatures. Tests were conducted to evaluate the cyclone's natural

length at simulated high temperatures. The inlet velocities, shown in table 5, correspond to what the syngas temperatures would be from FBG.

Table 5: Average inlet velocities of air at ambient conditions used to simulated inlet velocities of high temperature gases.

Average Inlet Velocity (m/s)	Related Density (kg/m^3)	Related Temperature (°C)
16.6	1.13	39
20.5	0.91	114
25.7	0.73	211
30.8	0.61	308
36.1	0.52	407
41.0	0.46	501
46.4	0.40	602

The Reynolds number from testing compared to FBG were calculated. A hydraulic diameter was used as the diameter of the inlet. The results from these calculations as shown in table 6. In order to represent the Reynolds number from FBG with a test system the inlet velocity of the cyclone would be below the conveying velocity of bio-char.

Table 6: Reynolds numbers from testing system and FBG.

Velocity (m/s)	Tests Reynolds Number	FBG Reynolds Number
16.5	29,300	29,300
20.5	36,400	25,700
25.7	45,600	22,300
30.8	54,700	19,800
36.1	64,000	17,800
41.0	72,800	16,400
46.4	82,400	15,100

The Reynolds number was also calculated for the MMD of the particles entering the cyclone. The Reynolds number was calculated for testing and FBG. A drag coefficient was calculated given the range of the Reynolds number. Results for these calculations, listed in table 7, were observed but not used for any further calculations.

Table 7: Particle Reynolds numbers from testing system and FBG.

Velocity (m/s)	Tests' Particle Reynolds Number	Drag Coefficient	FBG Particle Reynolds Number	Drag Coefficient
16.5	17	101	17	101
20.5	21	114	15	93
25.7	26	131	13	85
30.8	31	146	11	79
36.1	37	160	10	75
41.0	42	173	9	71
46.4	47	187	9	67

Cyclone Design

Using the TCD process, the diameter of the cyclone is a function of the airflow at STP (Parnell, 1996). The FBG bed in this study had a 15.2 cm (6-inch) diameter and was operated at a fuel-to-air ratio of 1:1. The energy loading was 23,900 MJ/m^2-hr (2.1 MMBtu/ft^2-hr). The airflow rate required for bed fluidization and the mass of gases produced from gasification were used to determine the cyclone diameter. In this FBG, 0.363 kg/min (0.8 lbs/min) of gas are produced from the biomass plus 0.454 kg/min (1 lb/min) of fluidizing air results in a total mass flow rate of 0.816 kg/min (1.8 lbs/min) of syngas. At STP, this mass flow rate is equivalent to 0.68 m^3/min (25 scfm). The optimal inlet velocity for a 1D3D cyclone was used for this cyclone. The resulting diameter for the cyclone, D, was 7.62 cm (3 inches), following equation 10 for sizing cyclones with the TCD process:

$$D = \sqrt{\frac{8Q}{V_i}} \tag{10}$$

where,

D = cyclone diameter (m),

Q = Airflow rate (m^3/s), and

V_i = Optimal design inlet velocity (1D3D = 16.3 m/s).

The configuration of the cyclone is shown in figure 5. The physical length of the barrel portion of the cyclone is equivalent to 20D. The idea behind constructing this cyclone was to be able to measure the natural length a multiple inlet velocities.

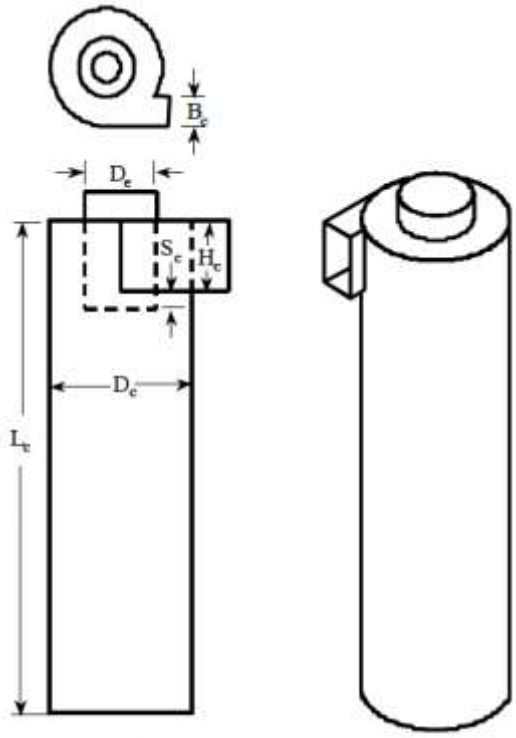

Figure 5: Cyclone configuration: Bc = Dc/4 Jc = Dc/4 De = Dc/2 Sc = Dc/8 Hc = Dc/2 Lc = 20Dc

Natural Length and Number of Turns

The natural length of the cyclone was measured by injecting a water and propylene glycol solution in the air prior to entering the cyclone. The solution would condense on the cyclone's wall causing the strands of the outer vortex and the turning point to become visible as seen in figure 6 and appendix A.

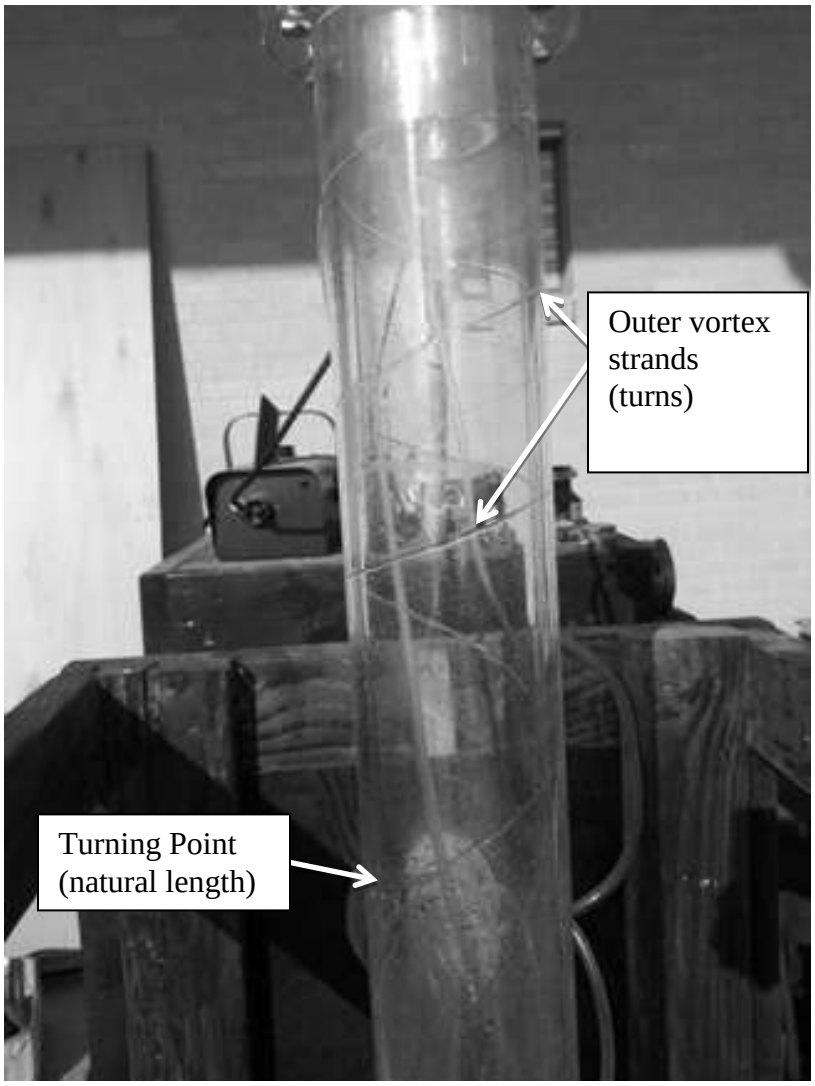

Figure 6: Visual test results used to determine the number of strands in the barrel cyclone's outer vortex and natural length.

A ring of liquid remained inside the cyclone once the walls of the cyclone dried. This ring was used to identify the location of the turning point of the outer vortex at the seven target inlet velocities. It was observed that as the walls of the cyclone dried the ring would travel further down the body of the cyclone. To assume a consistent coefficient of friction the ring position was not measured until the walls of the cyclone

were dry. The inlet velocity for each test was randomized in a complete block design with three replicates. The averaged results of these tests are shown in table 8.

Table 8: The natural Length was measured from the top of the cyclone to the ring of solution.

Average Inlet Velocity (m/s)	Average Measured Natural Length (cm)	Standard Deviation (cm)
16.6	22.9	0.3
20.5	23.2	0.3
25.7	23.8	0.3
30.8	24.3	0.5
36.1	25.7	0.3
41.0	28.6	0.6
46.4	30.5	1.3

The results from measuring the number of turns are shown in table 9. After consideration of these results, it appears that the strands shown by the solution on the wall of the cyclone might not represent the number of turns. The path the solution traveled down the wall of the cyclone could be a result of the momentum of liquid droplets flowing down the wall of the cyclone.

Table 9: The number of turns were recorded by counting the number of times the solution circled the body of the cyclone.

Average Inlet Velocity (m/s)	Number of Turns
16.6	2.5
20.5	2.9
25.7	3.4
30.8	3.5
36.1	3.6
41.0	3.8
46.4	4

Total Pressure Drop Model

The total pressure drop of the cyclone is calculated using the velocity at operating conditions and the cyclone specific K-value for a given velocity range. Using the TCD process the total pressure drop is determined with equation 6. To be able to calculate the total pressure drop across this cyclone for future use the K-value had to be determined. The cyclone was tested with air at ambient conditions. Data points measuring the pressure drop were collected every three second for 10 minutes. All pressure drop reading outside of three standard deviations from the average were removed. Cyclone pressure drop was recorded for the seven target inlet velocities. Tests were conducted in a randomized complete block design with four replicates. The total pressure drop was measured by recording the difference in the static pressure at the inlet and outlet of the cyclone as shown in table 10, while the velocity pressure was calculated following equation 7 and 8.

Table 10: Calculated constant K from tests at STP. The inlet and outlet velocity pressure were calculated to determine the K factor.

Inlet Velocity (m/s)	Total Pressure Drop (kPa)	Inlet Velocity Pressure (kPa)	Outlet Velocity Pressure (kPa)	Average K Value	Standard Deviation
16.5	1.1	0.2	0.1	4.6	±0.3
20.5	1.9	0.3	0.1	5.3	±0.1
25.7	3.1	0.4	0.2	5.5	±0.1
30.8	4.8	0.6	0.2	6.0	±0.1
36.1	6.7	0.8	0.3	6.1	±0.1
41.0	8.6	1.0	0.4	6.0	±0.1
46.4	10.6	1.3	0.5	5.8	±0.1

A trendline was used as a best fit for the data. A linear relationship was used to determine the K-value at a range of inlet velocities, as seen by equation 11:

$$K = \frac{V_i}{25.38} + 4.41 \tag{11}$$

where,

K = cyclone pressure drop factor, and

V_i = actual inlet velocity (m/s).

Natural Length Model

Wang published a model, shown previously in equation 4, for a theoretical approach to calculate the pressure drop across a cyclone that incorporated the inlet velocity and travel distance (Wang et al., 2002 and 2006). Her model utilized components of pressure drop. However, the pressure drop component due to the radial forces, in the cone section of the cyclone, was omitted from this model. The total pressure drop and three of the components (ΔP_e, ΔP_k, and ΔP_o) were calculated. The

portion of pressure drop loss due to friction was treated as the unknown variable. The results from equation 4 can be seen in table 11.

Table 11: Calculated total pressure drop and three of the components of pressure drop leaving friction loss as the unknown.

Total Pressure Drop (kPa)	Cyclone Entry Loss (kPa)	Kinetic Energy Loss (kPa)	Outlet and Inner Vortex Energy Loss (kPa)	Total Pressure Drop Due to Friction Loss (kPa)
1.1	0.2	0.1	0.1	0.8
1.8	0.2	0.1	0.2	1.2
2.9	0.4	0.2	0.3	2.0
4.4	0.6	0.3	0.4	3.1
6.2	0.8	0.5	0.6	4.4
8.4	1.0	0.6	0.7	6.1
11.0	1.3	0.7	0.9	8.0

Wang used a velocity of the strand in the outer vortex to determine the frictional forces (Wang, 2006). The theory behind this method is to account for the natural shape an air stream will form inside of a cyclone. The diameter of the strands in the outer vortex was determined with equation 12:

$$D_s = \frac{(D - D_o)}{2} \tag{12}$$

where,

D_s = diameter of the strand in the outer vortex (m),

D = diameter of the cyclone (m), and

D_o = diameter of the outlet of the cyclone (m).

The strand velocity was determined with equation 13:

$$V_s = Q / \frac{\pi {D_s}^2}{4} \quad (13)$$

where,

V_s = velocity of the strand in the outer vortex (m/s),

Q = volumetric airflow rate (m^3/s), and

D_s = diameter of the strand in the outer vortex (m).

Assuming a constant vertical trajectory of the outer vortex's strands, the frictional force was used to estimate the number of turns and natural length. The coefficient of friction was determined by calculating the Reynolds number, as shown in table 12. The friction factor, for Reynolds numbers less than 10^5 and in smooth pipes, was determined using equation 14 (ASHRAE Handbook, 1981):

$$f = 0.3164 / Re^{0.25} \quad (14)$$

where,

f =friction factor, and

Re = Reynolds number.

Table 12: The strand velocity was used in calculating the Reynolds number and solving for the friction factor.

Inlet Velocity (m/s)	Strand Velocity (m/s)	Airflow (m^3/s)	Simulated Temperature (°C)	Strand Reynolds Number	*Friction Factor f*
16.3	41.4	42.5	21	52,100	0.021
20.3	51.8	53.2	94	65,100	0.020
25.4	64.5	66.4	187	81,400	0.019
30.5	77.7	79.7	278	97,700	0.018
35.6	90.4	92.9	371	114,000	0.017
40.6	104	106	462	130,000	0.017
45.7	116	120	554	146,000	0.016

In this case, since the outer vortex's strands contact the cyclone wall on one side and the inner air stream on the other side, one-half of the frictional forces were used for the pressure drop calculation. Table 10 lists the friction factors for the cyclone at their respective design inlet velocities. The pressure drop due to friction in one turn was calculated with equation 15:

$$\Delta P_{f_i} = \left(f \frac{L}{D_s} VP_s\right)/2 \tag{15}$$

where,

$\Delta P_{f\,i}$ = frictional energy loss in one turn (kPa),

f = friction factor,

L = travel distance of one turn (L ≈ cyclone circumference) (m),

D_s = diameter of the strand in the outer vortex (m), and

VP_s = velocity pressure of the strand in the outer vortex (kPa).

The frictional force was used to estimate the number of turns and natural length. Dividing the total pressure drop due to friction, Table 9, by the pressure drop due to friction in one turn, equation 15, resulted in the number of turns and was calculated by equation 16:

$$N_e = \frac{k(VP_i + VP_o) - VP_i - (VP_i - VP_o) - 1.8VP_o}{f\frac{L}{D_s}VP_s/2} \tag{16}$$

where,

N_e = number of turns,

K = cyclone pressure drop constant (equation 11),

VP_i = velocity pressure of the inlet (kPa),

VP_o = velocity pressure of the outlet (kPa),

L = travel distance of one turn (L ≈ cyclone circumference) (m),

D_s = diameter of the strand in the outer vortex (m), and

VP_s = velocity pressure of the strand in the outer vortex (kPa).

Equation 17 is the equation used to calculate natural length and uses a constant slope of the outer vortex in the barrel portion a 1D3D cyclone (Wang et al., 2006):

$$L_N = \frac{N_e}{1.96} \tag{17}$$

where,

L_N = natural Length in cyclone diameters,

N_e = number of turns,

The results from equations 4, and 15-17 are listed in Table 13. These results were calculated with air at STP in order to compare the model to measured data.

Table 13: Calculated number of turns and natural length using equation 16 and 17.

Total Pressure Drop Due to Friction Loss (kPa)	Pressure Drop Due to Friction in One Turn (kPa)	Calculated Number of Turns	Natural Length (cm)
0.76	0.13	5.8	23.0
1.24	0.20	6.1	24.0
2.05	0.32	6.5	25.4
3.11	0.46	6.8	26.8
4.44	0.62	7.1	28.1
6.08	0.81	7.5	29.5
8.05	1.03	7.8	30.8

Comparison

The theoretical number of turns and natural length from this model were compared to results measured in visualization testing. Table 14 show the measured and theoretical number of turns for the cyclone. The theoretical number of turns shows a closer relationship to the number of turns in the TCD process for a 1D3D and a 2D2D cyclones at their optimal inlet velocities.

Table 14: Comparison of results from model and measured test. The model shows a closer relationship to the TCD 1D3D and 2D2D cyclones. The observations from measuring the number of turns do not represent the number of turns.

Target Inlet Velocity (m/s)	Number of Turns	Calculated Number of Turns
16.3	2.5	5.8
20.3	2.9	6.1
25.4	3.4	6.5
30.5	3.5	6.8
35.6	3.6	7.1
40.6	3.8	7.5
45.7	4	7.8

Table 15 shows the measured and calculated natural length for this cyclone.

Table 15: Results from the modeled and measured natural length.

Target Inlet velocity (m/s)	Average Measured Natural Length (cm)	Calculated Natural Length (cm)
16.3	22.9	23.0
20.3	23.2	24.0
25.4	23.8	25.4
30.5	24.3	26.8
35.6	25.7	28.1
40.6	28.6	29.5
45.7	30.5	30.8

A paired t-Test was used to statistical analysis the error in the measured and calculated data. An alpha of 0.05 was used to give a confidence interval of 95%. The null hypothesis was not rejected for the natural length, meaning that the model to predict natural length is significant. The model for number of turns was not significant to the measured data; however, it is possible that the visualization test did not represent the number of turns. Using the model 5.8 turns were calculated for an inlet velocity of 16.3 m/s. Parnell showed that a 1D3D cyclone has 6 turns at the same inlet velocity (Parnell, 1996).

CHAPTER IV

CYCLONE PERFORMANCE RESULTS AND DISCUSSION

Cyclone efficiency tests were conduct to determine the optimal cyclone design for removing bio-char from syngas produced in FBG. All tests were operated at ambient conditions with volumetric flow rates seen in FBG. Preliminary calibrations of the test system, figure 3, were performed.

The hypothesis includes that the natural length of the cyclone would increase as the inlet velocity increases. With that consideration, three vortex inverter locations, cyclone physical length, were chosen for testing the cyclones collection efficiency: 4D, 6D, and 8D. Each physical length represented a separate inlet velocity: 16.3 m/s for 4D vortex inverter location, 30.5 m/s for 6D vortex inverter location, and 45.7 m/s for 8D vortex inverter location. The location of the vortex inverter was based on estimations made from the model. All of the physical lengths were beyond the predicted natural lengths. In addition, at least one diameter was added to the estimation of the natural length to determine the location of the vortex inverter. It is also important to note that if the vortex inverter is located to close to the base of the cyclone a dramatic decrease in collection efficiency was observed (Luehrs, 2014).

The cyclones used in this research were referred to by the placement of the vortex inverter. If the vortex inverter location was at 4D the cyclone was named a 4D cyclone. To clarify, there was not a cone portion to these cyclones.

Testing Results

The filter housing was a lamination on the length of testing. It was observed that higher feed rates had a greater impact on the length of the test. The feed rate used for testing was 20 grams per minute. Following procedures from Luehrs (2014), three vortex inverter locations were used in determining the cyclone collection efficiency. The bio-char concentrations at each inlet velocity can be seen in table 16.

Table 16: The table shows the average inlet concentrations with a loading rate of 20 g/min at three inlet velocities for the cyclone.

Cyclone	Average Inlet Velocity (m/s)	Average Inlet Concentration (g/m^3)
4D	16.2	29.1 ±1.2
6D	30.3	12.6 ±1.6
8D	45.4	10.2 ±1.1

The exiting bio-char concentration was calculated for each cyclone and is show in table 17. The average exiting concentration decreased as the inlet velocity increased.

Table 17: Exiting bio-char concentration.

Cyclone	Average Outlet Velocity (m/s)	Average Exiting Concentration (g/m^3)
4D	10.3	0.69 ±0.19
6D	19.3	0.40 ±0.11
8D	28.9	0.32 ±0.09

The configuration of the cyclone is shown in figure 7. The vortex inverter had a diameter of 0.9D and a height of 0.45D. The vortex inverter was adjustable, allowing the ability to vary the physical length of the cyclone. The vortex inverter was placed below the estimated natural length in order to avoid compression of the strands in the outer vortex.

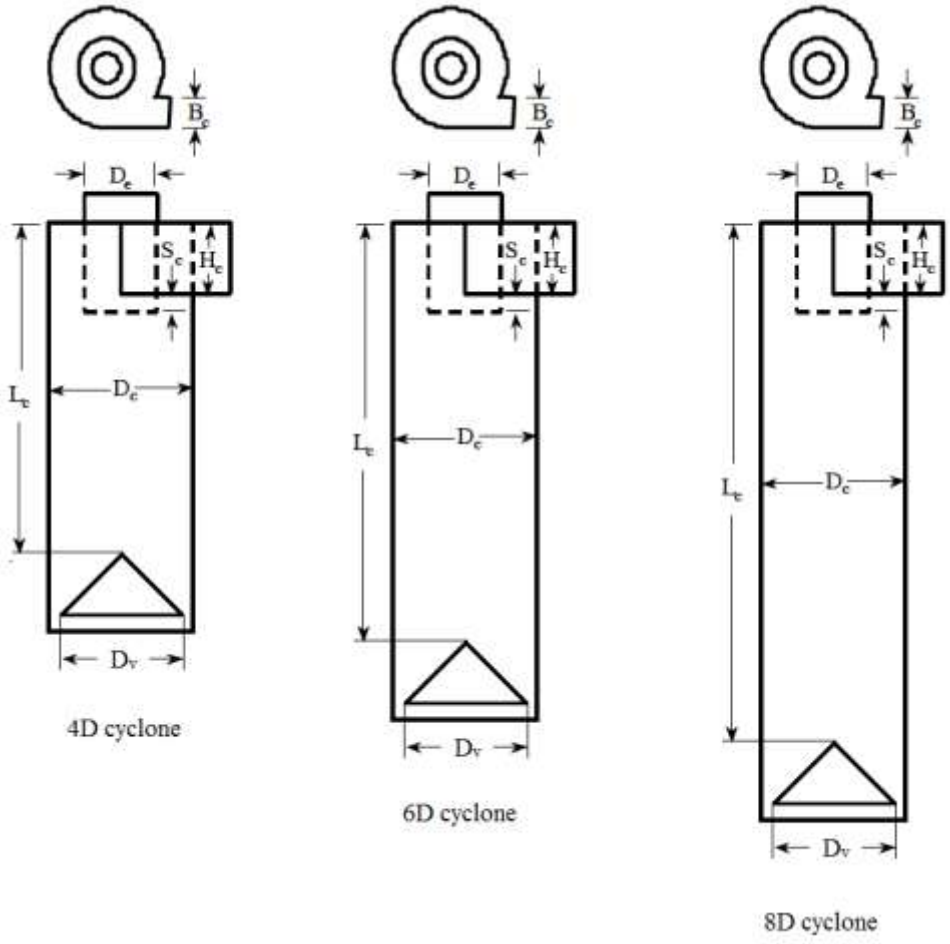

Figure 7: Cyclone configurations: $B_c = D_c/4$ $J_c = D_c/4$ $D_e = D_c/2$ $S_c = D_c/8$ $H_c = D_c/2$ $D_v = 0.9D_c$. The L_c varies for the inlet velocities: 16.3 m/s, $L_c = 4D_c$; 35.6 m/s, $L_c = 6D_c$; 45.7 m/s, $L_c = 8D_c$.

The PM to be used in this cyclone system is bio-char from the gasification of sweet sorghum. The bio-char's particle size distributions (PSDs) are best defined by lognormal distributions defined by mass median diameters (MMDs) and geometric standard deviations (GSDs) (Cooper and Alley, 2011). The lognormal fit of the measured and theoretical PSDs, obtained using the Coulter Counter, are shown in figure 8. The biochar used in this study has an MMD aerodynamic equivalent diameter (AED) of 27 μm, a geometric standard deviation (GSD) of 1.6 and a particle density of 2.1 g/cm^3.

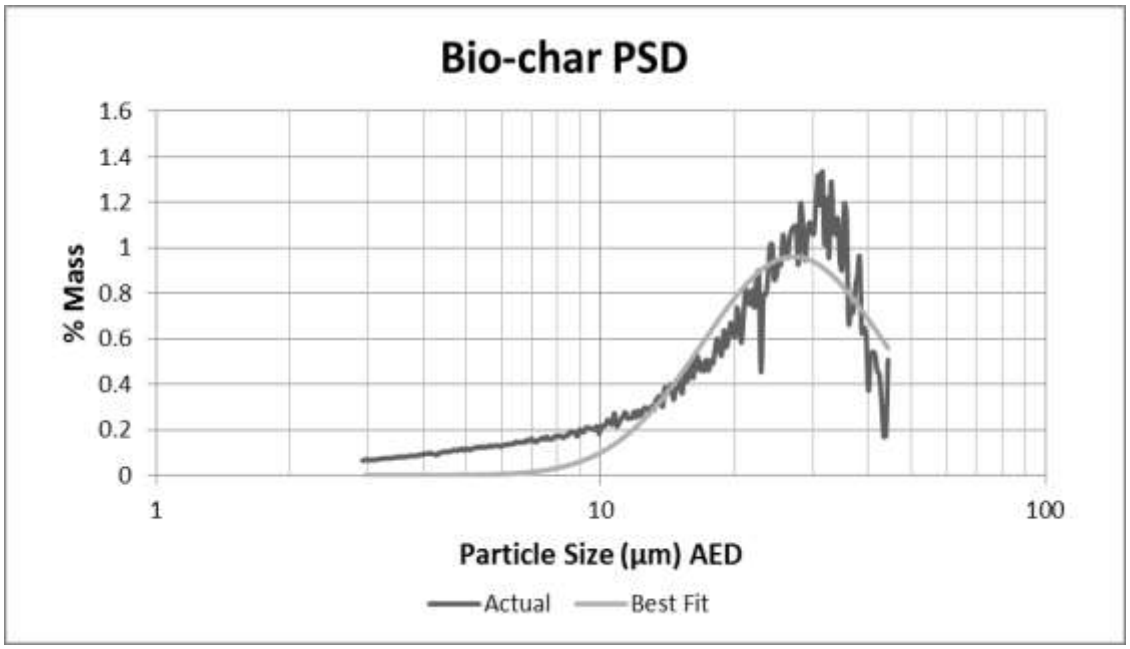

Figure 8: Particle size distributions of the bio-char used in this study. The plot illustrates the lognormal fit of the measured and theoretical PSDs obtained using the Coulter Counter.

The test system shown in figure 3 was designed and constructed to test cyclone collection efficiencies. Bio-char was fed into the airstream, prior to reaching the cyclone, at 20 grams per minute. Char entering the cyclone was either captured by the cyclone and fell into the char hopper or remained in the exiting airstream was it was captured in the filter assembly.

Collection efficiency was determined with equation 9. The range, average, and standard deviation of the collection efficiency at each level are listed in table 18. The results from each test are shown in appendix B. A 99% confidence interval from the mean was used to decide if data points were outliers.

Table 18: Average collection efficiency for the cyclones with three different vortex inverter locations.

Vortex Inverter	Number of Test	Average	Range
4D	8	97.8% ±0.6 %	97.3% to 98.8%
6D	8	96.9% ±0.8%	96.2% to 98%
8D	8	97.3% ±0.6%	96.6% to 98%

The collection efficiency for each of the vortex inverter locations are shown in Figures 9-11.

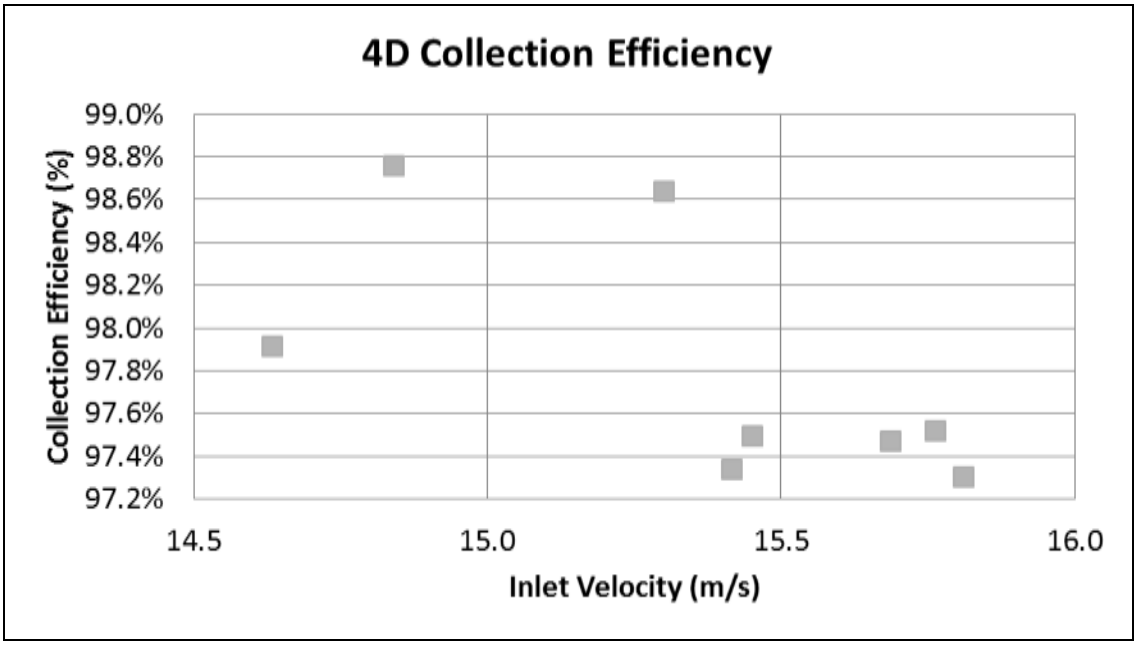

Figure 9: Collection efficiency for the cyclone with the vortex inverter located at 4D. The average collection efficiency for this cyclone was 97.8%.

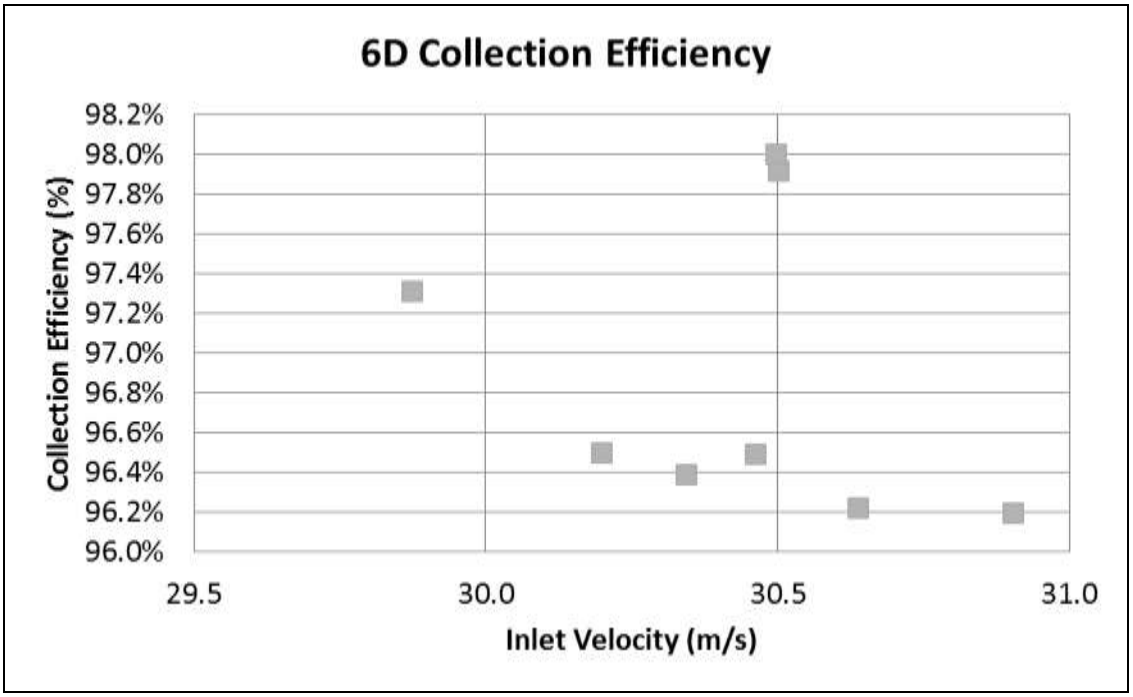

Figure 10: Collection efficiency for the cyclone with the vortex inverter located at 6D. The average collection efficiency for this cyclone was 96.9%.

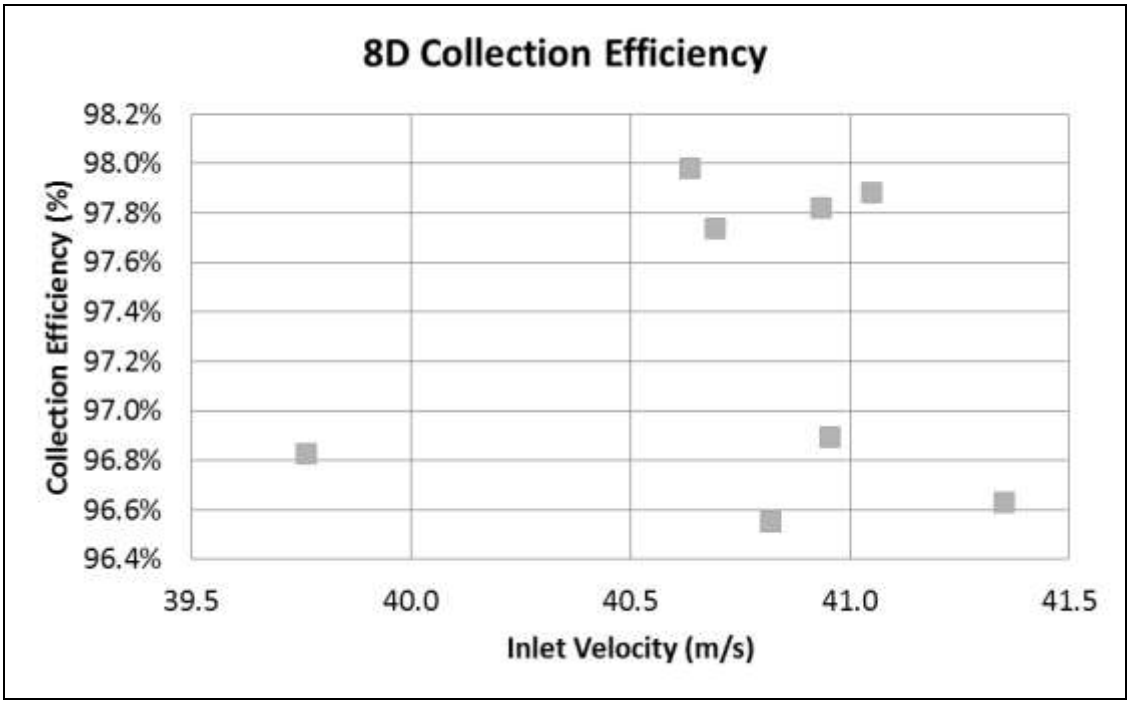

Figure 11: Collection efficiency for the cyclone with the vortex inverter located at 8D. The average collection efficiency for this cyclone was 97.3%.

Cutpoint and Slope

In the TCD process, the performance of a cyclone is defined by its fractional efficiency curve (FEC), which indicates the efficiency with which a cyclone collects particles of a given size (Faulkner et al., 2008). An ideal FEC is characterized a lognormal distribution defined by the cutpoint and slope. An expected cutpoint was calculated for this cyclone at each inlet velocity using the TCD cutpoint equation 5. The number of turns used in calculating the cut point was calculated from equation 16. Results from the cut point equation are listed in table 19. The calculated cutpoint was less than 1 µm for two of the target inlet velocities. It is not feasible for a cutpoint of this

value to represent a cyclone with a FEC. Other methods to determine the cutpoint were reviewed.

Table 19: The TCD calculated cutpoint for three different inlet velocities. Number of turns was calculated by using equation 16.

Inlet Velocity (m/s)	Number of Turns	AED Cutpoint (µm)
16.3	5.8	1.12
30.5	6.8	0.75
45.7	7.8	0.58

The collection efficiency from cyclone testing and the calculated TCD cutpoint were used to determine the slope for this cyclone. The results from this method are listed in table 20 for each cyclone. The results from each test are shown it Appendix C. A lognormal FEC was used to back calculate the slope from the collection efficiency and cutpoint as shown in equation 18 (Faulkner et al., 2008):

$$FEC(d_p, d_{50}, slope) = \frac{1}{d_p[ln(slope)]\sqrt{2\pi}} exp\left[\frac{-(lnd_p - lnd_{50})^2}{2[ln(slope)]^2}\right] \quad (18)$$

where,

FEC(d_p, d_{50}, slope) = collection efficiency of particle with diameter d_p,

d_{50} = cyclone cutpoint, which is the particle size corresponding to 50% collection efficiency, and

slope = slope of the FEC.

Table 20: The slope was determined by back calculating a FEC given the efficiency from testing and cutpoint. The cutpoint was calculated using the TCD cutpoint equation 5.

Cyclone	Inlet Velocity	Efficiency	Cutpoint	Slope	d15.9	d84.1
4D	15.4	97.8%	1.1	3.7	0.3	3.3
6D	30.4	96.9%	0.8	5.5	0.1	7.2
8D	40.8	97.3%	0.6	6.0	0.1	10.4

The table 20 shows that there was a range of averaged cutpoints from 1.12 to 0.58 μm with a slope of 3.72 to 5.99 for the 4D and 8D cyclones receptively. Graphical representations of each cyclone are shown in the FEC's in figure 12. It is understood that as the inlet velocity increases the cut point will decrease (Cooper and Alley, 2011). However, there is no historical cyclone work that show a slope that matches the slopes found in this approach.

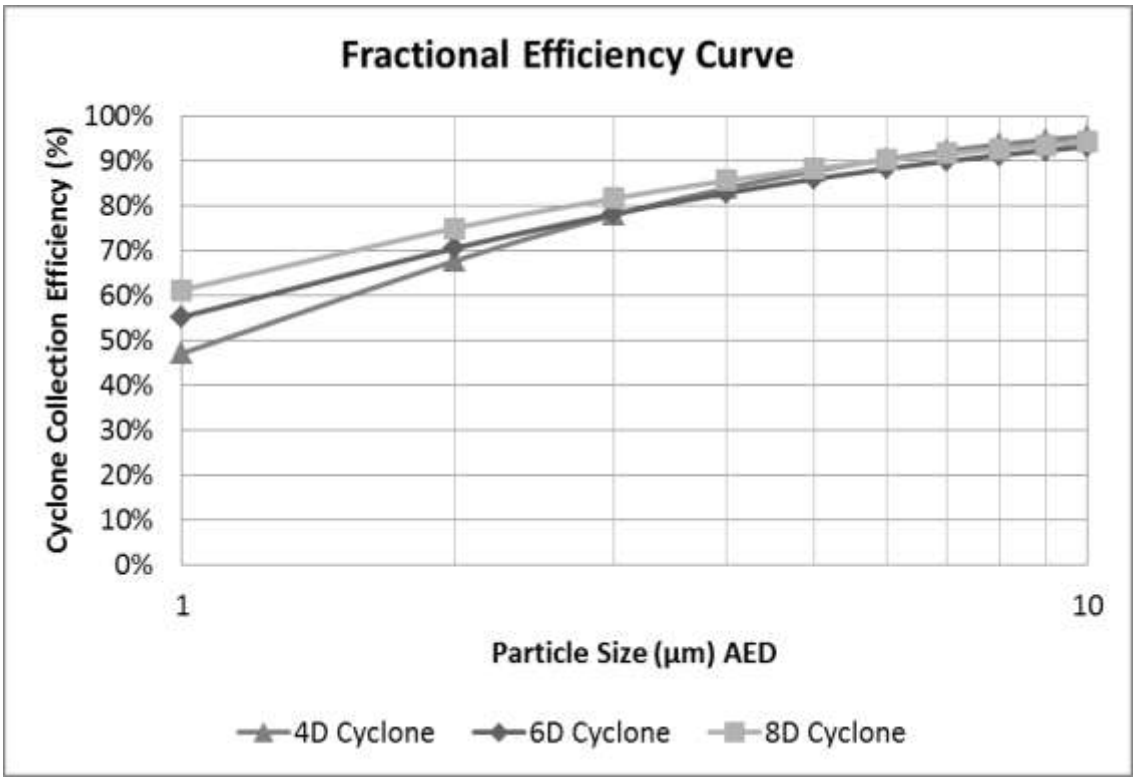

Figure 12: FEC for three cyclones: 4D, 6D, and 8D. d_{50} found using TCD cutpoint equation. As you can see this FEC does not resemble the FEC in figure 4.

Another way to calculate the cutpoint and slope would be from using the PSD of the exiting concentration leaving the cyclone. Glass fiber filters were used to capture the exciting bio-char from the cyclone. A methanol solution was used to remove the accumulated bio-char without damaging the filter. In a PSD 50% of the particles are above and below the MMD. An average of the PSD for the three different cyclones is shown in figure 13.

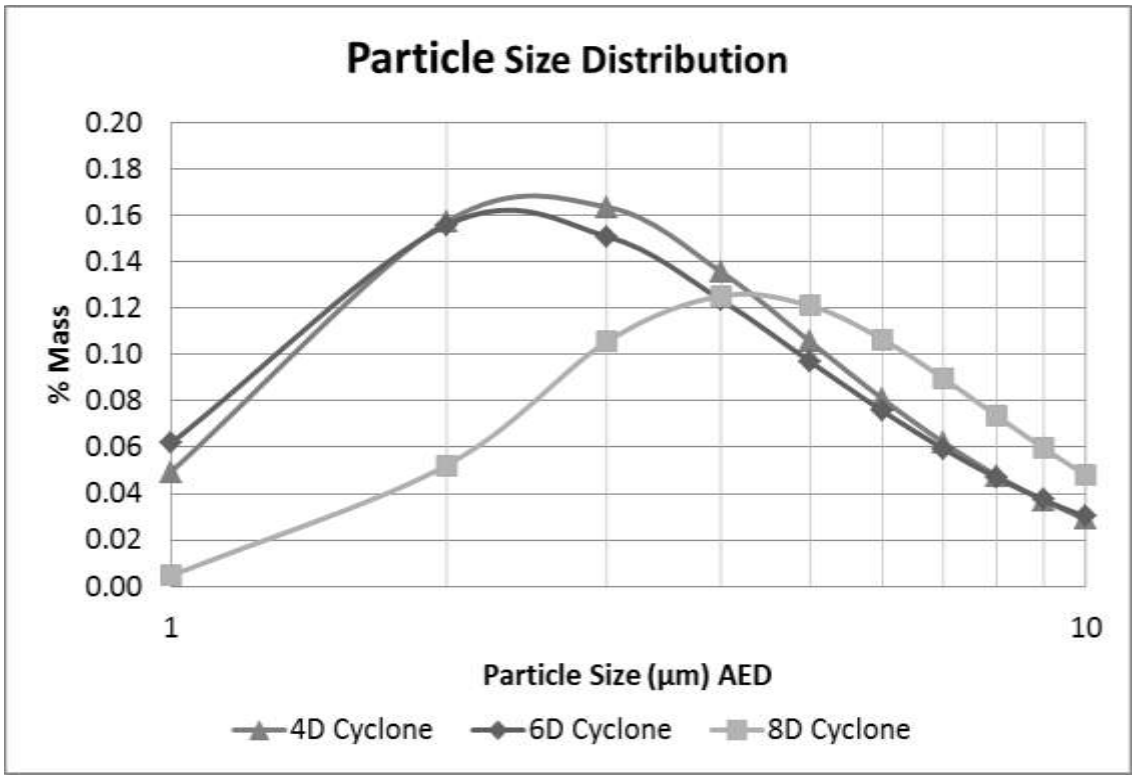

Figure 13: PSD for three cyclones: 4D, 6D, and 8D. The peak of each test would be the cutpoint by following this method.

The peak of each PSD represents the AED MMD of the particles for each test. The particles leaving the cyclone had a MMD less than 5 µm. A FEC was calculated by using the MMD as the cutpoint. In this approach the slope was determined by back calculating a FEC knowing the efficiency of each test and using the MMD for the cutpoint. The FEC for the same three tests are shown in figure 14 and the results for this approach are shown in table 21. The results from each test are shown it appendix D.

Table 21: The Coulter Counter results for the PSD of the exiting gas stream. MMD's are represented in AED and are believed to be a representation of the cutpoint for the cyclone. .

Cyclone	Inlet Velocity	Efficiency	Cutpoint	Slope	d15.9	d84.1
Average 4D	15.4	97.8%	3.91	2.30	1.7	0.6
Average 6D	30.4	96.9%	4.08	2.49	1.7	0.7
Average 8D	40.8	97.3%	5.85	1.97	3.2	0.4

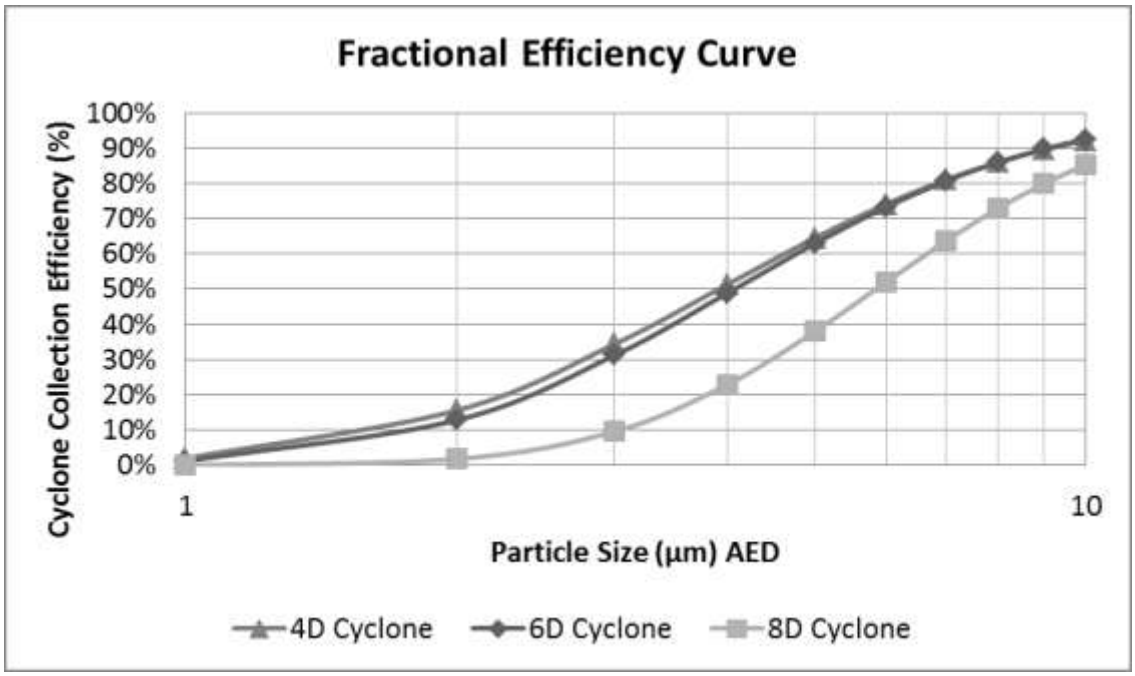

Figure 14: FEC for three cyclones: 4D, 6D, and 8D.

The results from this approach did not show any correlation between the MMD of the exiting bio-char as the cutpoint and the collection efficiency. The cutpoints and slopes had variation that could not be explained by an increase in the cyclones inlet velocity. The cyclone's slope could not be described by this approach.

Another method to calculate the cut point for this cyclone is by using Faulkner's model. He found that the cutpoint of a cyclone could be determined based on the diameter of the cyclone. The relationship between the cyclone diameter and cutpoint is shown with equation 19:

$$d_{50} = aD^{b} \tag{19}$$

where,

d_{50} = cutpoint (µm),

D = cyclone diameter (cm),

a = 2.855, and

b = 0.076.

Applying this equation to this cyclone resulted in a calculated cutpoint of 3.33 µm. Using this cutpoint, and the efficiencies found in testing, the slope was determined again by using a FEC model. The results from this approach can be seen in table 22. The results from each test are shown it appendix E.

Table 22: The slope was determined by back calculating a FEC given the efficiency and cutpoint. The cutpoint was determined by using equation 19.

Cyclone	Inlet Velocity	Efficiency	Cutpoint	Slope	$d_{15.9}$	$d_{84.1}$
4D Average	15.4	97.8%	3.33	1.80	0.5	1.9
6D Average	30.4	96.9%	3.33	2.07	0.6	1.6
8D Average	40.8	97.3%	3.33	1.96	0.6	1.7

An average slope of 1.94 was determined to be the best fit for this cyclone. A cutpoint of 3.33 µm and a slope of 1.94 were used to calculate the efficiency for this

cyclone and tested to be significant at a 95% confidence level. A FEC to represent this cyclone is displayed in figure 15.

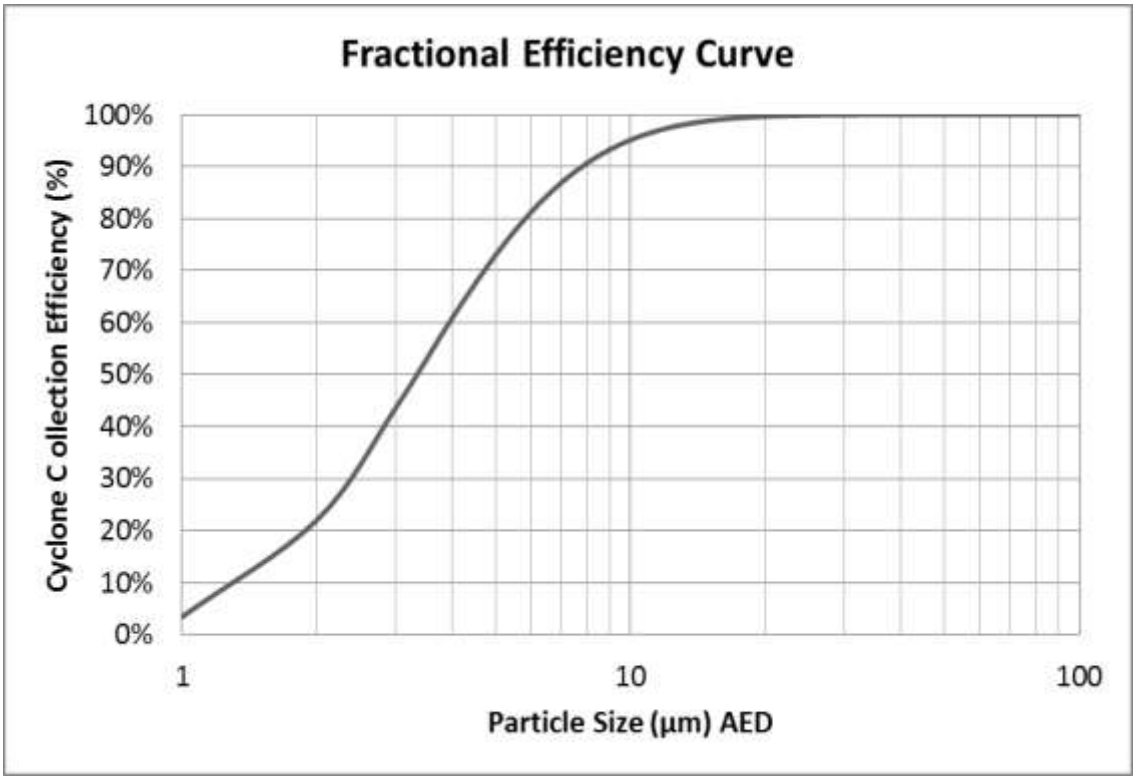

Figure 15: The FEC for all three cyclones with the d_{50} cutpoint equal to 3.33 and a slope of 1.94.

Pressure Drop

The pressure drop across the cyclone was recorded for each test. The results were grouped by the vortex inverter location and shown in figure 16 – 18.

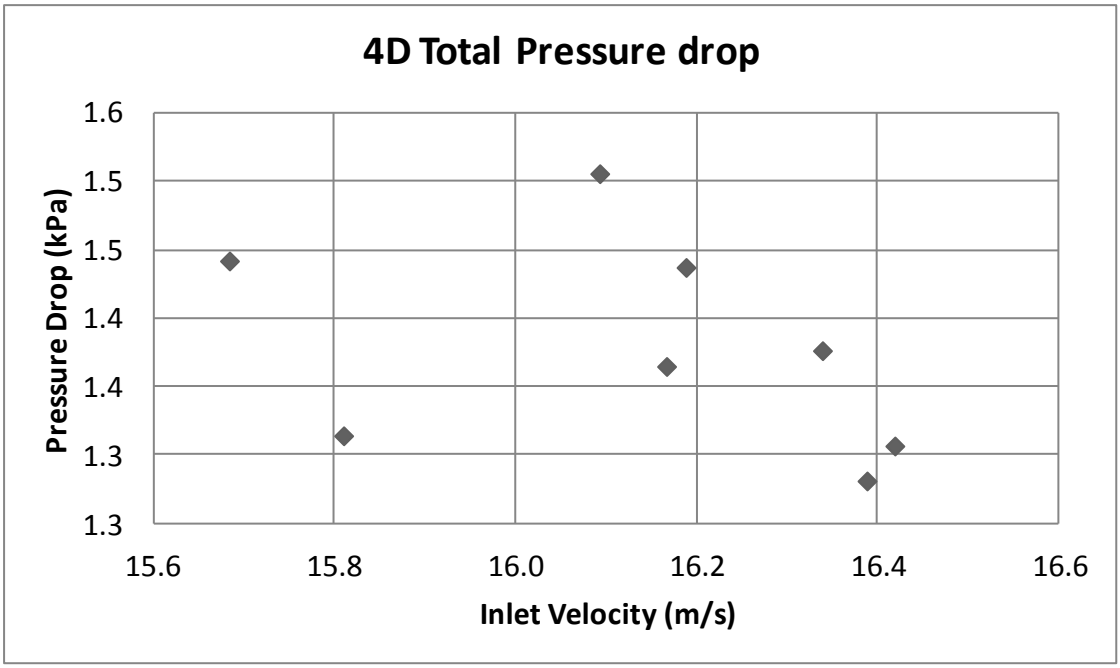

Figure 16: The pressure drop for each 4D cyclone test.

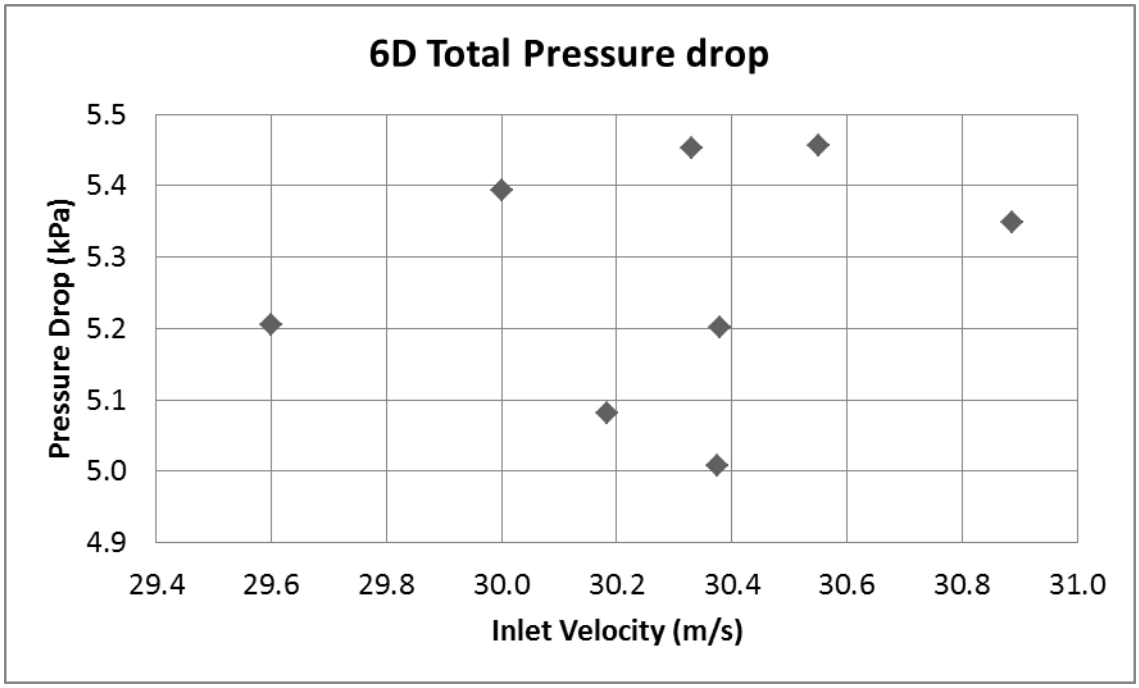

Figure 17: The pressure drop for each 6D cyclone test.

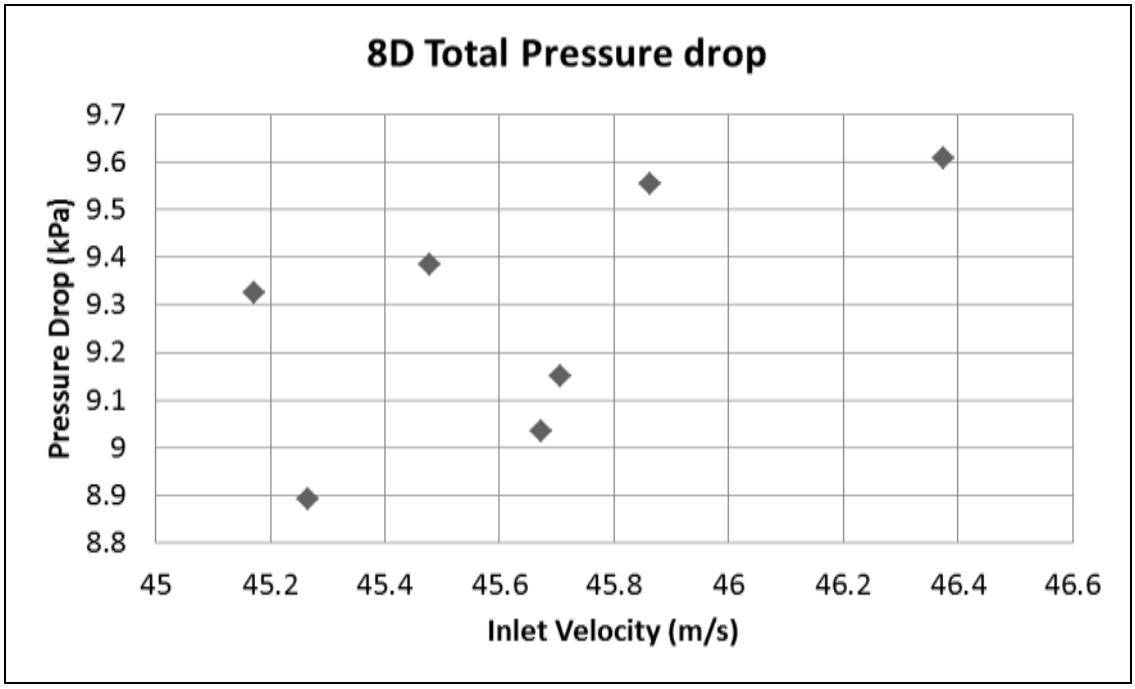

Figure 18: The pressure drop for each 8D cyclone test.

The measured pressure drop was compared to the calculated pressure drop, from equation 6 & 11, in figure 19. The calculated pressure drop was statistically significant at a confidence level of 95%.

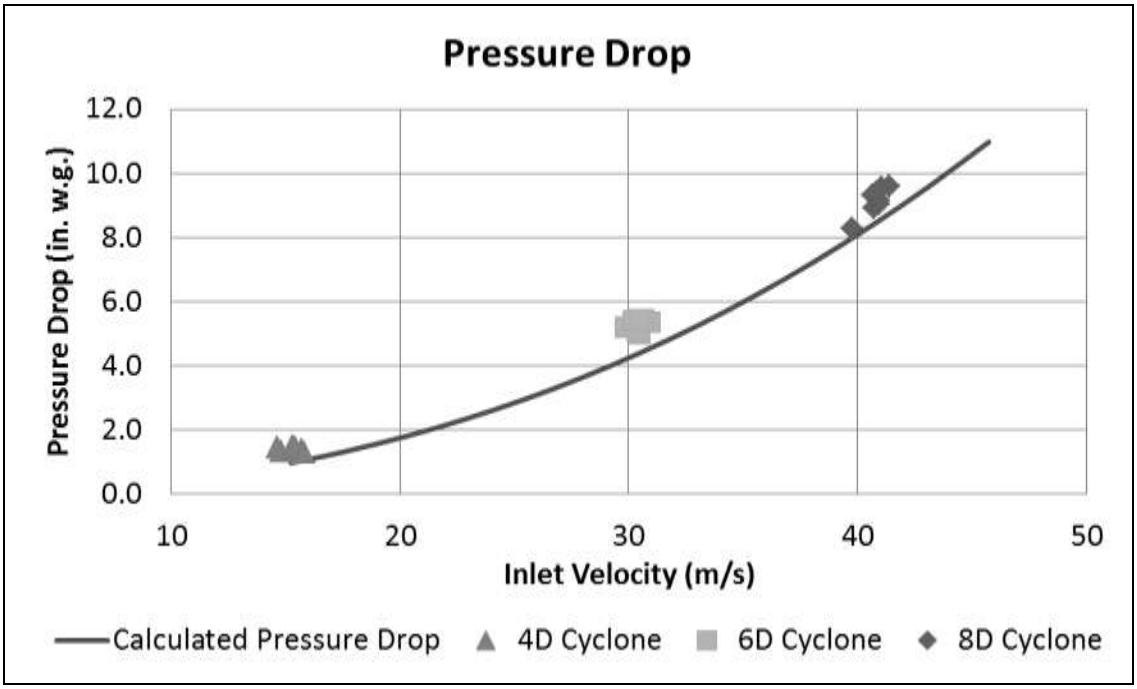

Figure 19: Total pressure drop across the cyclones compared to the calculated pressure drop.

CHAPTER V

CONCLUSION

The models used in this research accurately predicted the cyclones' natural length. The method used to measure the number of turns was flawed, and the model was used to calculate the number of turns instead. The natural length and number of turns were both found to be a function of the cyclones inlet velocity and can be determined as follows:

- Cyclone should be sized to the optimal TCD design velocity at STP of 16.3 m/s (3,200 fpm).
- The total pressure drop for this cyclone is calculated with equations 6-8 and 11.

- The total pressure drop and K – value is a function of inlet velocity.

- The number of turns can be determined as a function of the total pressure drop in equation 16.
- The natural length of the cyclone can be determined as a function of the total pressure drop and inlet velocity at actual conditions with equation 17

Results from this research suggested that the cyclones collection efficiency could be calculated. It seems that by extending the cyclones physical length there was no interference between the strands. The same cutpoint and slope were found to be significant at all inlet velocities. The cutpoint can be determined with equation 19 at all inlet velocities tested. The slope was determined to remain constant at all velocities

tested. The AED cutpoint for this cyclone is equal to 3.33 µm with a slope of 1.94.

The method used to calculate the pressure drop across the cyclone could be calculated by using the TCD process. The actual inlet velocity should be used to calculate the velocity pressure of the inlet and the outlet of the cyclone. The K value is a function of inlet velocity at actual conditions. Theoretical pressure drop for FBG at actual conditions (high temperatures) are shown in figure 20.

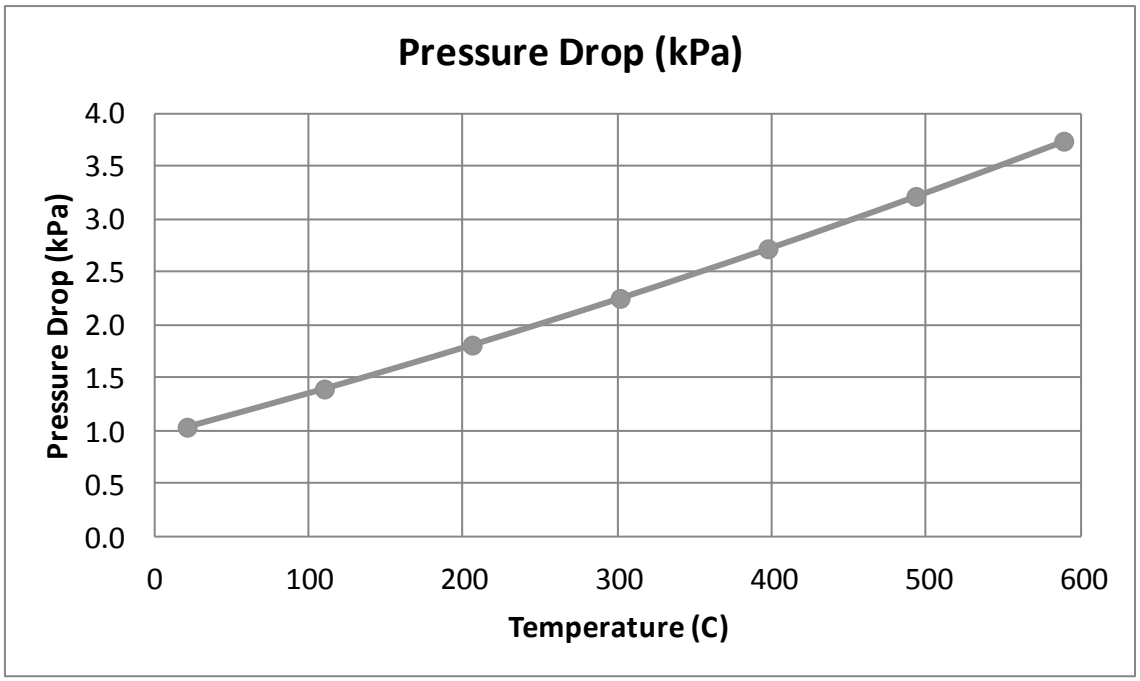

Figure 20: Theoretical pressure drop for high temperature gases.

Future cyclones designed with this TCD approach for high temperature gases should follow the following steps:

1. Airflow from actual to standard:

   - $Q = Q_{actual} \frac{\rho_{standard}}{\rho_{actual}}$

2. Cyclone diameter:
    - $D = \sqrt{8Q/16.3}$
3. Vortex inverter location:
    - $N_e = V_i/16.9 + 4.74$
    - $L_N D = N_e/1.96$
4. Total pressure drop:
    - $\Delta P = K(VP_i + VP_o)$
    - $K = V_i/25.38 + 4.41$
5. Cyclone collection efficiency:
    - Cutpoint, $d_{50} = 2.86D^{0.076}$
    - Slope = 1.94

Future work is still needed to determine the carbon content of the bio-char in the exiting gas stream. The fine particles not captured by the cyclone could have a high carbon content. If that is the case then the exiting bio-char could be consumed into an ICE. The carbon content for different particle ranges could help to determine if the particles exiting the cyclone could be considered as fuel.

REFERENCES

Alexander, R. M. 1949. Fundamentals of cyclone design and operation. In Proceedings Australasian Institute of Mining and Metallurgy. (New Series) 152-3: 203-228.

American Society of Heating, Refrigerating and Air Conditioning Engineers Fundamentals. 1981. ASHRAE/ANSI standard 55-81: Fluid Flow. ASHRAE, Atlanta, Georgia.

Barth, W. 1956. Design and Layout of the Cyclone Separator on the Basis of New Investigations. Brenn. Warme Kraft 8: 1-9.

Capareda, S. C., C.B. Parnell, Jr. and W. A. LePori. 2010. Biomass Thermochemical Conversion System. U.S. Provisional Patent Serial No. 61,302,001 Texas A&M University.

Capareda, S. and C.B. Parnell, Jr. 2007. Fluidized Bed Gasification of Cotton Gin Trash for Liquid Fuel Production. Proceedings of the 2007 Beltwide Cotton Conferences, New Orleans, Louisiana.

Cooper, C.D. and F.C. Alley. 2011. Air Pollution Control: A Design Approach. Prospect Heights, Illinois: Waveland Press.

Dietz, P. W. 1981. Collection Efficiency of Cyclone Separators. American Institute of Chemical Engineers Journal 27: 888.

Faulkner, W.B., M.D. Buser, D.P. Whitelock, and B.W. Shaw. 2008. Effects of Cyclone Diameter on Performance of 1D3D Cyclones: Cut Point and Slope. Transactions of the ASABE 51(1): 287-292.

First, M. W. 1950. Fundamental Factors in the Design of Cyclone Dust Collectors. PhD diss. Cambridge, Massachusetts, Harvard University.

Hoffmann, A. C., R. de Jonge, H. Arends and C. Hanrats.1995. Evidence of the ‘Natural Vortex Length’ and its Effect on the Separation Efficiency of Gas Cyclones. Filtration & Separation 32.8: 799-804.

Lapple, C. E. 1951. Processes Use Many Collector Types. Chemical Eng. 58(5): 144-151.

LePori, W.A. and C.B. Parnell, Jr. 1989. System and Process for Conversion of Biomass into Usable Energy. U.S. Patent No. 4848249

Lepori, W.A., and E.J. Soltes. 1985. Thermochemical Conversion for Energy and Fuel. In Biomass Energy: A Monograph, 9-75. E. A. Hiler and B.A. Stout, eds. College Station, Texas, Texas A&M University Press.

Luehrs, D.R., C.B. Parnell, Jr. and McGee, R.O. 2014. Reducing PM Concentrations in Simulated High Temperature Gas Streams. Proceedings of the 2014 Beltwide Cotton Conference, National Cotton Council. New Orleans, Louisiana.

Maglinao, A. L. Jr. 2013. Development of a Segregated Municipal Solid Waste Gasification System for Electrical Power Generation. PhD diss. College Station, Texas: Texas A&M University, Department of Biological and Agricultural Engineering.

Parnell, C.B., Jr. 1985. Systems Engineering of Biomass-Fueled Energy Alternatives. In Biomass Energy: A Monograph, 213-248. E. A. Hiler and B.A. Stout, eds. College Station, Texas, Texas A&M University Press.

Parnell, C.B. Jr. 1996. Cyclone Design For Air Pollution Abatement Associated With Agricultural Operations. Proceedings of the 1996 Beltwide Cotton Production Conferences, National Cotton Council. Nashville, Tennessee.

Saucier, D.S. 2013. Cyclone Performance for Reducing Biochar Concentrations in Syngas. M.S. Thesis. College Station, Texas: Texas A&M University, Department of Biological and Agricultural Engineering.

Shepherd, C. B., and C. E. Lapple. 1939. Flow Pattern and Pressure Drop in Cyclone Dust Collectors. Industrial and Eng. Chemistry 31(8): 972-984.

Shepherd, C. B., and C. E. Lapple. 1940. Flow Pattern and Pressure Drop in Cyclone Dust Collectors. Industrial and Eng. Chemistry 32: 1246-1248.

Simpson, S. and C.B. Parnell, Jr. 1995. New Low Pressure Cyclone design for Cotton Gins. Proceedings of the 1995 Beltwide Cotton Conferences, National Cotton Council, Memphis, Tennessee.

Stairmand, C. J. 1949. Pressure Drop in Cyclone Separators. Industrial and Eng. Chemistry 16(B): 409-411.

Texas Cotton Ginners Association. 2006. TCGA Gin Operating Cost Survey. Texas Cotton Ginners Association, Austin, Texas

Tullis, A. W., B.W. Shaw, C.B. Parnell, Jr., P.P. Buharivala, M.A. Demny and S.S. Flannigan. 1997. Design and Analysis of the Barrel Cyclone. Proceedings of the 1997 Beltwide Cotton Conferences, Memphis, Tennessee.

Wang, L., Parnell, C. B., and Shaw, B. W. 2002. Study of the Cyclone Fractional Efficiency Curves. Agricultural Engineering International: The CIGR Journal of Scientific Research and Development, Vol. IV.

Wang, L. 2004. Theoretical Study of Cyclone Design. PhD diss. College Station, Texas: Texas A&M University, Department of Biological and Agricultural Engineering.

Wang, L., C.B. Parnell, Jr., B.W. Shaw and R.E. Lacey. 2006. A Theoretical Approach for Predicting Number of Turns and Cyclone Pressure Drop. Transactions of the ASABE 49(2): 491–503.

APPENDIX A

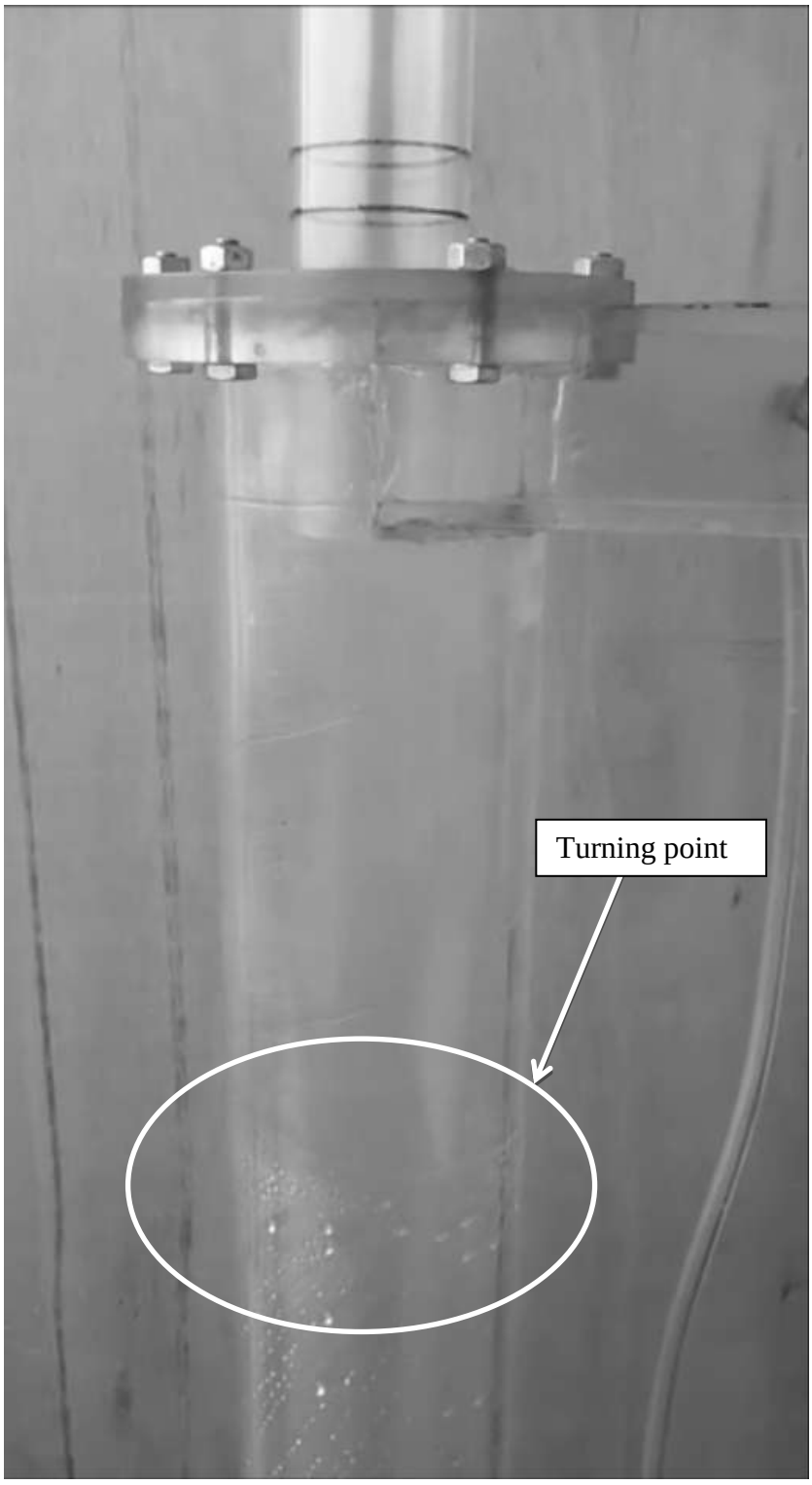

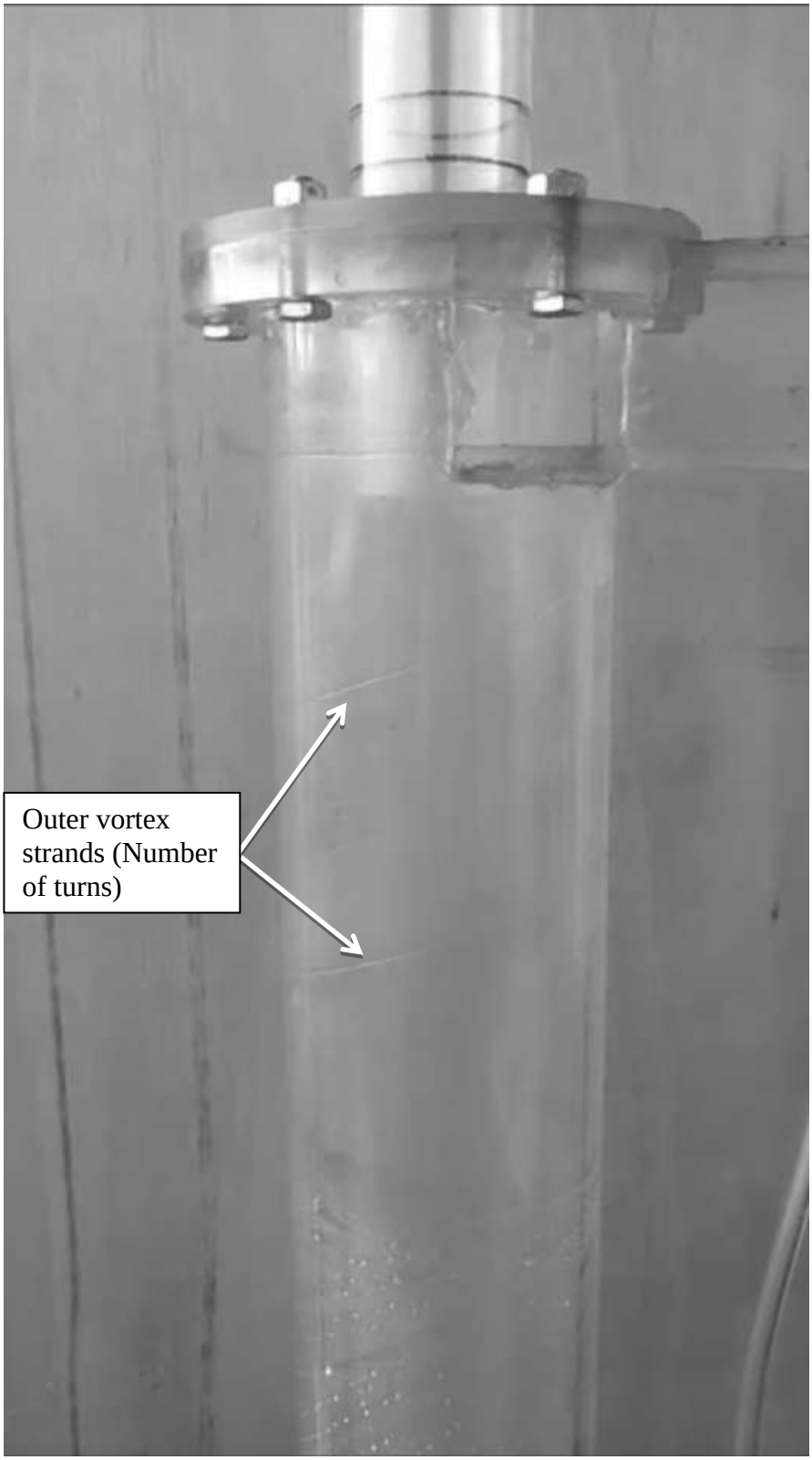
Outer vortex strands (Number of turns)

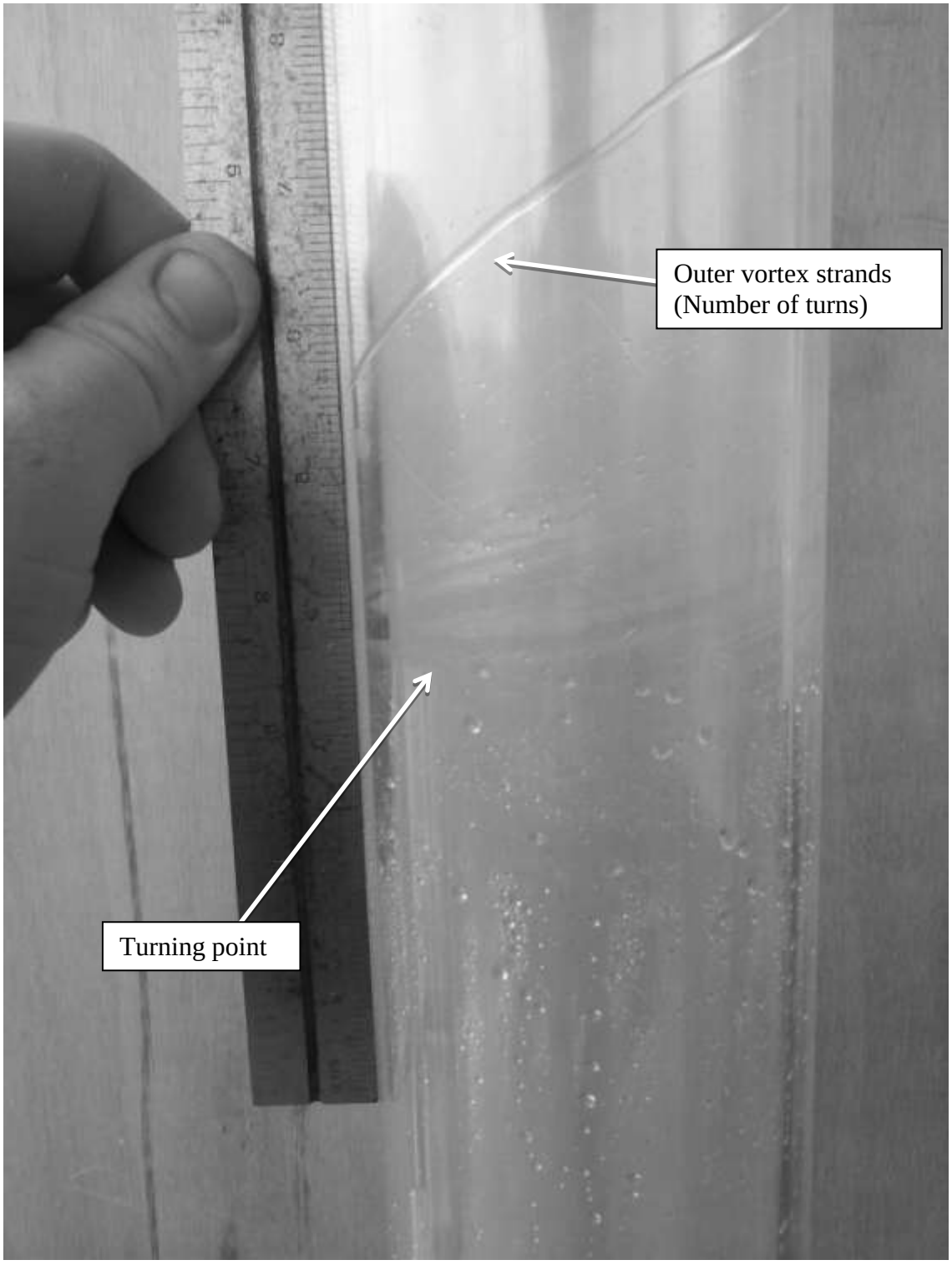
Outer vortex strands
(Number of turns)
Turning point

APPENDIX B

Appendix B: Tests results for cyclone collection efficiency testing.

Test #	Vortex Inverter Location	Mass Feed Rate (g/m^3)	Inlet Velocity (m/s)	Total Pressure drop (kPa)	Efficiency
2	4D	19.8	14.8	5.3	98.8%
3	4D	19.6	14.6	5.8	97.9%
2.1	6D	17.6	30.5	20.9	97.9%
3.1	6D	18.0	30.5	20.1	98.0%
8	6D	15.0	30.3	20.4	96.4%
11	8D	18.9	39.8	33.2	96.8%
12	8D	17.7	40.7	35.7	97.7%
13	4D	20.2	15.3	6.0	98.6%
14	4D	20.2	15.7	5.5	97.5%
15	4D	19.5	15.4	5.5	97.3%
17	6D	20.3	30.9	21.5	96.2%
18	6D	16.0	29.9	20.9	97.3%
19	8D	18.9	40.9	36.3	97.8%
20	8D	20.7	40.6	37.5	98.0%
21	8D	19.2	41.0	38.4	97.9%
22	6D	16.7	30.6	21.9	96.2%
23	6D	16.5	30.2	21.7	96.5%
24	6D	12.6	30.5	21.9	96.5%
25	4D	22.4	15.8	5.1	97.5%
26	4D	21.4	15.5	5.8	97.5%
27	4D	20.6	15.8	5.2	97.3%
28	8D	25.1	41.0	36.7	96.9%
29	8D	20.6	41.4	38.6	96.6%
30	8D	20.6	40.8	37.7	96.6%

APPENDIX C

Appendix C: The slope was determined by back calculating a FEC given the efficiency from testing and cutpoint. The cutpoint was determined using the TCD cutpoint equation.

Test #	Inlet Velocity	Efficiency	Cutpoint	Slope	d15.9	d84.1
2	14.8	98.8%	1.13	3.07	0.37	2.71
3	14.6	97.9%	1.14	3.63	0.31	3.19
13.1	15.3	98.6%	1.12	3.17	0.35	2.82
14.1	15.7	97.5%	1.12	3.96	0.28	3.55
15	15.4	97.3%	1.12	4.03	0.28	3.59
25	15.8	97.5%	1.11	3.93	0.28	3.53
26	15.5	97.5%	1.12	3.93	0.29	3.51
27	15.8	97.3%	1.11	4.07	0.27	3.66
2.1	30.5	97.9%	0.76	4.58	0.16	6.06
3.1	30.5	98.0%	0.76	4.51	0.17	5.97
8	30.3	96.4%	0.76	5.89	0.13	7.77
17	30.9	96.2%	0.75	6.1	0.12	8.14
18	29.9	97.3%	0.77	5.07	0.15	6.62
22	30.6	96.2%	0.75	6.08	0.12	8.07
23	30.2	96.5%	0.76	5.78	0.13	7.60
24	30.5	96.5%	0.76	5.81	0.13	7.68
11	39.8	96.8%	0.59	6.4	0.09	10.9
12	40.7	97.7%	0.58	5.49	0.11	9.50
19	40.9	97.8%	0.58	5.42	0.11	9.42
20	40.6	98.0%	0.58	5.23	0.11	9.04
21	41.0	97.9%	0.57	5.36	0.11	9.34
28	41.0	96.9%	0.58	6.41	0.09	11.1
29	41.4	96.6%	0.57	6.72	0.08	11.8
30	40.8	96.6%	0.58	6.86	0.08	11.9

APPENDIX D

Appendix D: The slope was determined by back calculating a FEC given the efficiency from testing and cutpoint. The cutpoint was determined using the MMD from the exiting bio-char.

Test #	Inlet Velocity	Efficiency	Cutpoint	Slope	d15.9	d84.1
2	14.8	98.8%	3.76	2.09	1.80	0.55
3	14.6	97.9%	3.82	2.31	1.65	0.61
13.1	15.3	98.6%	4.11	2.04	2.01	0.50
14.1	15.7	97.5%	4.01	2.34	1.71	0.58
15	15.4	97.3%	3.96	2.40	1.65	0.61
25	15.8	97.5%	3.98	2.35	1.69	0.59
26	15.5	97.5%	3.7	2.45	1.51	0.66
27	15.8	97.3%	3.96	2.40	1.65	0.61
2.1	30.5	97.9%	3.31	2.50	1.32	0.76
3.1	30.5	98.0%	3.40	2.44	1.39	0.72
8	30.3	96.4%	3.65	2.74	1.33	0.75
17	30.9	96.2%	4.66	2.39	1.95	0.51
18	29.9	97.3%	5.93	1.88	3.16	0.32
22	30.6	96.2%	3.42	2.90	1.18	0.85
23	30.2	96.5%	4.83	2.28	2.12	0.47
24	30.5	96.5%	3.41	2.83	1.21	0.83
11	39.8	96.8%	8.27	1.54	5.37	0.19
12	40.7	97.7%	3.20	2.61	1.23	0.82
19	40.9	97.8%	5.84	1.82	3.22	0.31
20	40.6	98.0%	5.21	1.95	2.67	0.37
21	41.0	97.9%	6.17	1.74	3.55	0.28
28	41.0	96.9%	8.65	1.47	5.87	0.17
29	41.4	96.6%	4.54	2.35	1.93	0.52
30	40.8	96.6%	4.88	2.27	2.15	0.46

APPENDIX E

Appendix E: The slope was determined by back calculating a FEC given the efficiency and cutpoint. The cutpoint was determined by using Faulkner's cutpoint equation for cyclone diameter (equation 19).

Test #	Inlet Velocity	Efficiency	Cutpoint	Slope	$d_{15.9}$	$d_{84.1}$
2	14.8	98.8%	3.33	1.48	0.44	2.25
3	14.6	97.9%	3.33	1.78	0.53	1.87
13.1	15.3	98.6%	3.33	1.53	0.46	2.18
14.1	15.7	97.5%	3.33	1.91	0.57	1.74
15	15.4	97.3%	3.33	1.95	0.59	1.71
25	15.8	97.5%	3.33	1.9	0.57	1.75
26	15.5	97.5%	3.33	1.9	0.57	1.75
27	15.8	97.3%	3.33	1.96	0.59	1.70
2.1	30.5	97.9%	3.33	1.78	0.53	1.87
3.1	30.5	98.0%	3.33	1.76	0.53	1.89
8	30.3	96.4%	3.33	2.2	0.66	1.51
17	30.9	96.2%	3.33	2.25	0.68	1.48
18	29.9	97.3%	3.33	1.96	0.59	1.70
22	30.6	96.2%	3.33	2.24	0.67	1.49
23	30.2	96.5%	3.33	2.17	0.65	1.53
24	30.5	96.5%	3.33	2.17	0.65	1.53
11	39.8	96.8%	3.33	2.09	0.63	1.59
12	40.7	97.7%	3.33	1.84	0.55	1.81
19	40.9	97.8%	3.33	1.81	0.54	1.84
20	40.6	98.0%	3.33	1.76	0.53	1.89
21	41.0	97.9%	3.33	1.79	0.54	1.86
28	41.0	96.9%	3.33	2.07	0.62	1.61
29	41.4	96.6%	3.33	2.14	0.64	1.56
30	40.8	96.6%	3.33	2.18	0.65	1.53